

**Technische Universität München**  
**Lehrstuhl für Kommunikationsnetze**  
Prof. Dr.-Ing. Wolfgang Kellerer

## **Bachelor's Thesis**

Data Aggregation in LTE-A Uplink Through  
Clustering

Author:	Buitrago Méndez, Arturo
Address:	Türkenstrasse 58a 80799 München Germany
Matriculation Number:	03646899
Supervisor:	Mikhail Vilgelm, M.Sc.
Begin:	01. January 1900
End:	01. January 2000

With my signature below, I assert that the work in this thesis has been composed by myself independently and no source materials or aids other than those mentioned in the thesis have been used.

München, 14.10.2016

---

Place, Date

---

Signature

This work is licensed under the Creative Commons Attribution 3.0 Germany License. To view a copy of the license, visit <http://creativecommons.org/licenses/by/3.0/de>

Or

Send a letter to Creative Commons, 171 Second Street, Suite 300, San Francisco, California 94105, USA.

München, 14.10.2016

---

Place, Date

---

Signature

# Contents

<b>Contents</b>	<b>3</b>
<b>1 Introduction</b>	<b>5</b>
<b>2 Background</b>	<b>7</b>
2.1 Random Access and its Limitations . . . . .	7
2.2 Device-to-Device . . . . .	8
2.3 Clustering . . . . .	9
<b>3 Implementation</b>	<b>11</b>
3.1 Generation and distribution of UEs . . . . .	11
3.2 Path loss (attenuation) . . . . .	13
3.2.1 Manhattan grid . . . . .	13
3.2.2 Line-of-sight . . . . .	15
3.2.3 Non-line-of-sight . . . . .	15
3.3 Shadow fading . . . . .	17
3.4 Random access procedure and interference . . . . .	18
3.5 Clustering Algorithms . . . . .	20
3.5.1 LEACH . . . . .	21
3.5.2 Complete-Link Clustering . . . . .	22
3.5.3 Single-Link Clustering . . . . .	23
3.5.4 Ward's Method . . . . .	23
<b>4 Results</b>	<b>25</b>
4.1 Evaluation methodology . . . . .	25
4.1.1 Percentage of UEs connecting to eNB . . . . .	27
4.1.2 Mean channel utilization rate . . . . .	27
4.1.3 Total resource efficiency . . . . .	28
4.1.4 Mean UE drop ratio . . . . .	28
4.2 LEACH . . . . .	29
4.3 Hierarchical Algorithms . . . . .	35
4.3.1 Complete-Link . . . . .	35
4.3.2 Single-Link . . . . .	35

<i>CONTENTS</i>	4
4.3.3 Ward's Method . . . . .	37
4.4 Comparison . . . . .	39
4.4.1 Percentage of UEs connecting to eNB . . . . .	39
<b>5 Conclusions and Outlook</b>	<b>43</b>
<b>A Notation and Abbreviations</b>	<b>44</b>
<b>List of Figures</b>	<b>46</b>
<b>List of Tables</b>	<b>47</b>
<b>Bibliography</b>	<b>48</b>

# Chapter 1

## Introduction

One of the most promising directions the field of communication networks has explored in the last years has been the Internet of Things (IoT) [SRI<sup>+</sup>15]. An explosion in the capability of everyday objects to connect and communicate with each other via wireless networks promises to mightily expand the boundaries hitherto explored by technology. It also promises to place an almost unmanageable amount of stress into the technologies and infrastructure already in place [PCZZ16].

One of the proposed approaches to ameliorate the overload of connections originating from hundreds of devices to a base station is the grouping of the signals via different algorithms into clusters, which then transmit the aggregated information in one single signal to the rest of the network [LWW<sup>+</sup>14]. This is compounded by the prospective boons that Device-to-Device (D2D) communication promises when integrated into the network [FDM<sup>+</sup>12].

Although many such algorithms have been proposed, especially coming from the field of Wireless Sensor Networks (WSNs) where data aggregation is much more a matter of course [ATN14], there has been woefully little attention paid to the viability of such mechanisms in comparison to one another in a scenario conforming to the standards and circumstances of LTE-A and D2D communication. These kind of considerations are specially relevant when considering the prospective arrival of the IoT, the emergence of concepts such as smart grids and smart cities and the prospect of 5G as the next generation of technology that will have to deal with these issues [DGK<sup>+</sup>13].

In this work we will be restricting ourselves to exactly this framework: an urban, highly dense scenario, where traffic inside clusters is observed and measured, while accounting for interference both within and without these structures. The clustering algorithms used will all be single-hop, i.e. with only one aggregation stage before connecting to the base station. The models used, when possible, will all adhere to the modern standards of LTE-A, including its procedure for random access and collision resolution. Monitoring the traffic at the base station itself, or other kinds of more complex algorithms are outside the scope of this thesis.

This thesis aims to create a coherent and realistic simulation scenario for the evaluation of traffic within an increasingly important scenario for LTE-A, that of a highly dense, highly interconnected city. This simulation's usefulness will not be restricted to this thesis but will be able to be incorporated into future work in the field, by its author or otherwise. This work also intends to quantify the adequacy of different clustering schemes in aggregating data effectively and alleviating congestion in the network. This will allow future research to better focus its efforts on algorithms that are viable. Finally, this work's contribution dovetails into the larger scope of work done in the institute at which it was written in the areas of D2D and Random Access.

The rest of the thesis will be organized as follows: First, a background section will introduce the topic and situate it within the state of research and technological standards. Next, the implementation chapter will detail the steps taken to create an appropriate simulation environment for our investigation. Finally, the results will be presented and discussed. The conclusion will recapitulate the outcomes and identify opportunities for improvement and future research.

# Chapter 2

## Background

### 2.1 Random Access and its Limitations

The necessity of the expansion of the existing standards of wireless networks for the effective handling of large numbers of Machine Type Communications (MTC) had already been identified by the 3GPP early in the implementation of Long Term Evolution (LTE) as a standard in [3rd11]. As explained in [LAAZ14], a large amount of problems arise with increasingly large amounts of devices connecting to the Base Station (BS) or Evolved Node B (eNodeB) mostly due to the Random Access (RA) procedure that has to be initiated with every connection.

RA procedures occur when a device intends to utilize resources on the Physical Uplink Shared Channel (PUSCH), but has not been given access to the Physical Uplink Control Channel (PUCCH) by the appropriate eNB, which is needed for a scheduling request. As described in [Cox12], the User Equipment (UE) then sends a random access preamble to trigger the procedure, in order to gain the desired access, see figure 2.1.

This preamble is chosen randomly from an available set generated with a Zadoff-Chu mathematical sequence and transmitted on the Physical Random Access Channel (PRACH). The eNB then solves any possible collisions that may occur from devices transmitting with the same preamble, granting access to some while ordering others to back off for a certain amount of time. If no access grant is given after several tries, the transmission is considered to have failed.

When a large amount of these connections are initiated in a short time frame, the contention resolution procedures cannot deal with them in a timely manner and many of them are dropped or delayed significantly, waiting for an opportunity to synchronize with the eNodeB, as shown in [PCZZ16]. This scenario occurs most often either because the transmission times are highly correlated or just due to the large number of devices in a given area. Both of these circumstances, both in isolation and in conjunction, will be very

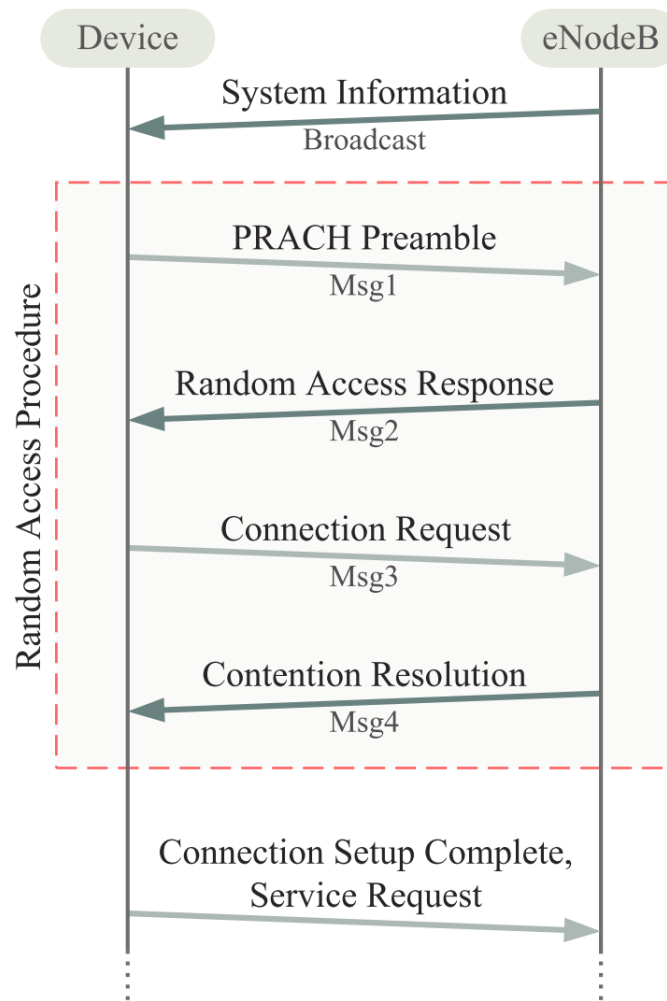


Figure 2.1: Detail of the Random Access Procedure, [LAAZ14]

ordinary occurrences in Internet of Things (IoT) and Smart City applications, concepts speculated to be made possible in the future by Device-to-Device communications.

## 2.2 Device-to-Device

One of the technologies that enable the great amount of enthusiasm in the field about the future of interconnected devices is Device-to-Device communication. D2D, as the wireless standard for direct communication between UEs in LTE-A is called, offers a means to expand the existing wireless cellular network to accommodate these type of transmissions. D2D has been widely regarded as one of the technologies heralding a new world of higher interconnectivity and will be a key component in 5G.



D2D communication's potential contributions have been documented widely and continued to be researched to this day. Some of the most popular applications include:

- Proximity-based services, such as social networking or gaming
- Public safety and emergency communication applications
- Local media transmission for businesses or advertisement
- Vehicle-to-Vehicle communication
- Localized Peer-to-Peer file transfer

In all these applications, D2D presents potential gains in capacity, data rate, latency and load reduction when compared to similar applications that would have to access the network directly before performing their function. This thesis attempts to explore the viability of specific applications of this type of communication as well as quantify some of the aforementioned gains, while taking into account some of the challenges they face, such as interference from other devices.

In this thesis, we work with D2D connections being allocated resources from within the cellular network's bandwidth. These are then kept apart from those used by normal cellular communication after the initial allocation, however. For details on this point, please refer to section 3.4.

## 2.3 Clustering

Many approaches have been suggested for the improvement of the circumstances described in section 2.1, as summarized succinctly in [LAAZ14], mostly dealing with the improvement of the RA procedures or an expansion of the standards for the Random Access Channel (RACH). Another viable alternative, as presented in a variety of papers ([WHS12a],[LWW<sup>+</sup>14],[WSH<sup>+</sup>13],[LQL13]) is the clustering of transmitting devices. This approach aims to reutilize the coding and frequency resources within a given set of UEs for different ends, such as decreasing the load on the eNB, increasing the coverage area of the network or minimizing the power consumption of the units involved.

Clustering works by designating devices, called Cluster Heads (CH) that act as relays between the different UEs in a certain area and the eNB or a further Cluster Head by aggregating the data sent to it and relaying it. This aggregation can occur simply by gathering the data over a period of time and transmitting the same information in one long message, as in [SOIJ15], or through actual elimination of data redundancy, as contemplated in [RCCM15].

The Cluster Heads themselves are often dedicated gateways, as utilized in [NXW11] or [SOIJ15] and have been utilized especially in Wireless Sensor Networks with some fre-

quency. Another, very promising approach to creating clusters is the integration of D2D communication to eliminate the need for dedicated Cluster Heads and enable dynamic cluster forming depending on the circumstances experienced by the network. This type of clustering scheme promises to bring much needed flexibility to the creation of these structures, since they do not necessitate much investment in additional infrastructure, nor much prior information about the density of devices. D2D communications bring many benefits, both for the user and the network, but also raise several issues that have not been yet properly investigated so far, see [KK14a]. As devices utilize the same shared resources in a constrained space, interference becomes more of an issue as devices elect to transmit their messages in the same bandwidth. This topic of inter-cluster interference due to reuse of resources and its effects on possible D2D connections is of great interest to this thesis.

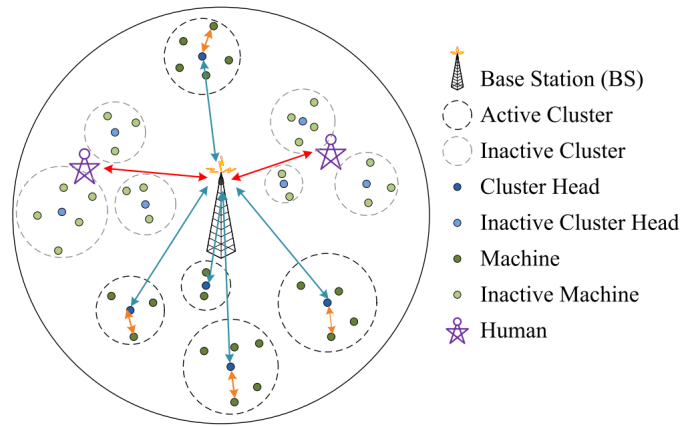


Figure 2.2: Example of D2D Clustering in a network [WSH<sup>+</sup>13]

As mentioned earlier, this sort of application is specially intriguing in the case of highly dense Smart Cities and the IoT. Despite the promising vistas offered by this technology, there is a dearth of research concerning this specific scenario, be it a comparison of different clustering schemes or even the detailed simulation of one clustering schemes with varying parameters. Although detailed surveys of algorithms exist, such as [JYZ09] or [ATN14], they mostly center around description and classification. This thesis is meant to alleviate this lack of exploration. Not only will different clustering schemes be analyzed and compared fairly, they will also be scrutinized under different criteria, allowing for an assessment of their viability. This will hopefully give a direction to future possible research in this area, by highlighting some of them as viable or others as not viable at all.

The next chapters will explain in detail the steps taken to create the simulation environment as well as a presentation and evaluation of the results it yielded.

# Chapter 3

## Implementation

As mentioned in the preceding chapters, the development of the simulation environment was as much a goal of this thesis as any; we seek to lay the groundwork for further investigation in this field with a credible system that reproduces faithfully the conditions found in a dense, urban environment with many devices capable of accessing the network. Ideally, the work presented here will be refined and will continue to be used on investigations in this area.

For the creation of such a testing environment, five elements were recognized as of utmost importance to the validity of the tests and the author sought to implement them accordingly. In the following, they will be presented with detail, justifying the sources of the models and the parameter choices made.

The aforementioned elements are:

- Generation and distribution of UEs
- Path loss (attenuation)
- Shadow fading
- Random access procedure and interference
- Clustering algorithms

The actual simulations, as well as the measures used to quantify the relative performance of each algorithm are presented in chapter 4.

### 3.1 Generation and distribution of UEs

Often called a “completely” random process, a Poisson process is a process where every event is stochastically independent of all other points in it, see [Kee16]. This generation

process is common in investigations about the performance of networks, as eloquently expressed by [Kee] In our case, the Poisson-distributed random variable are the number of points in the bounded region we are investigating. The distribution is described by the following probability mass function:

$$f_X(x \text{ points in region}) = \frac{e^{-\lambda} \lambda^x}{x!} \quad (3.1)$$

By providing the  $\lambda$  above, often called mean density ([Kee16]), we can adjust the expected amount of points generated in a given area. In order to evaluate the robustness of different algorithms, the tests were made with a variety of  $\lambda$  values. The generated amount of points are then distributed in the given area with a uniform distribution, where both the  $x$  and  $y$  value are distributed along the appropriate axis. In both cases, the *Python* package *NumPy* was utilized for the realization of the random distributions.

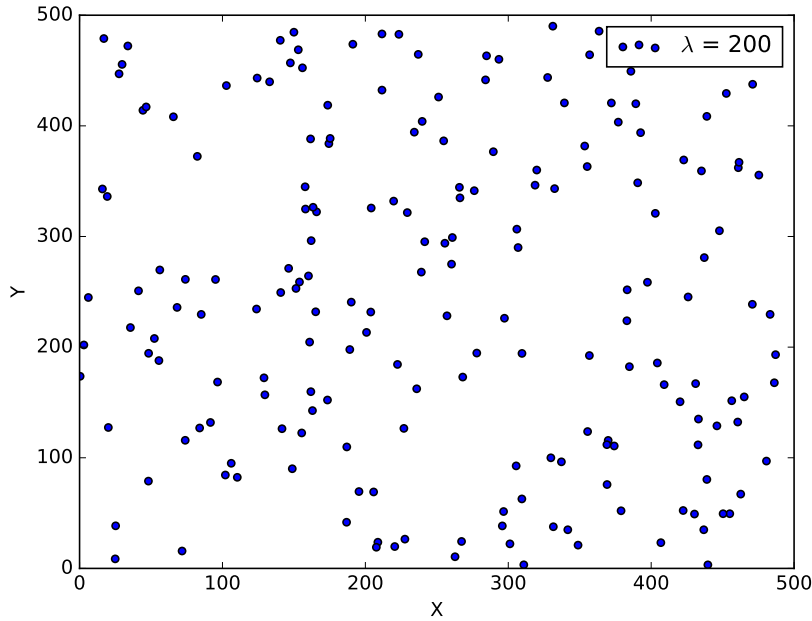


Figure 3.1: Example of a PPP with  $\lambda = 200$

Thus we have generated the number and position of all our UEs according to a Poisson point process (PPP).

## 3.2 Path loss (attenuation)

Whenever transmission between devices is being investigated, loss due to attenuation as the signal propagates through space is an unavoidable topic. Distance degrades electromagnetic waves in terms of power in any real system and any simulation that does not reflect this phenomenon is simply not valid.

In search of the best documented and most forward-looking models available, we settled on the use of METIS (Mobile and wireless communications Enablers for the Twenty-twenty Information Society), a EU Project that seeks to promote the definition of 5G mobile technologies. Its channel model, presented in its deliverables ([Mw15]) was especially insightful.

For the purposes of this thesis, the Stochastic Model, a “geometry-based stochastic channel model”, was chosen for the way it lined up with our own goals, especially when it came to level of detail and complexity. Their figures are based on previous efforts by 3GPP studies to model these same phenomena. Due to the highly dense, urban system we are investigating, propagation scenario number one, “Urban Micro” was selected. Due to the constraints of this thesis, we narrowed our focus on Outside-to-Outside (O2O) connections, although the integration of Outside-to-Inside (O2I) could be a feature of future research.

When calculating the attenuation for a given path between two devices, there emerge two distinct cases, depending on whether there are any significant obstacles between the two of them: Line-of-sight (LOS) and Non-line-of-sight (NLOS).

### 3.2.1 Manhattan grid

In order to determine whether a given link is a LOS or NLOS link, we need information about the obstacles present in the path between the two. In our case, we don’t consider objects like cars and people explicitly, but rather account for all such minor objects and reflections they might create with a stochastic model (see 3.3). Buildings, on the other hand, represent such massive, nigh-impenetrable objects that we must contemplate them concretely.

The preferred method mentioned in the METIS deliverables is the use of a “Manhattan-like” grid, meaning a city-layout comprised of rectangular blocks criss-crossed by wide streets. To determine both the size and the overall layout of our Manhattan Grid, we again turn to the extensive work done by METIS. The measurements with which their relevant models were tested were run in Madrid, with a grid of around 500 meters of both length and width. We homogenized the scenario by having exclusively square blocks, but maintained both the street width and the general dimensions. We also fixed the position of the eNodeB exactly at the middle of the grid for those clustering algorithms that needed its position.

Parameter	Value
Grid Dimensions	500 m $\times$ 500 m
Block Width	110 m
Block Length	110 m
Street Width	20 m
eNB position	(250 m, 250 m)

Table 3.1: Manhattan grid parameters

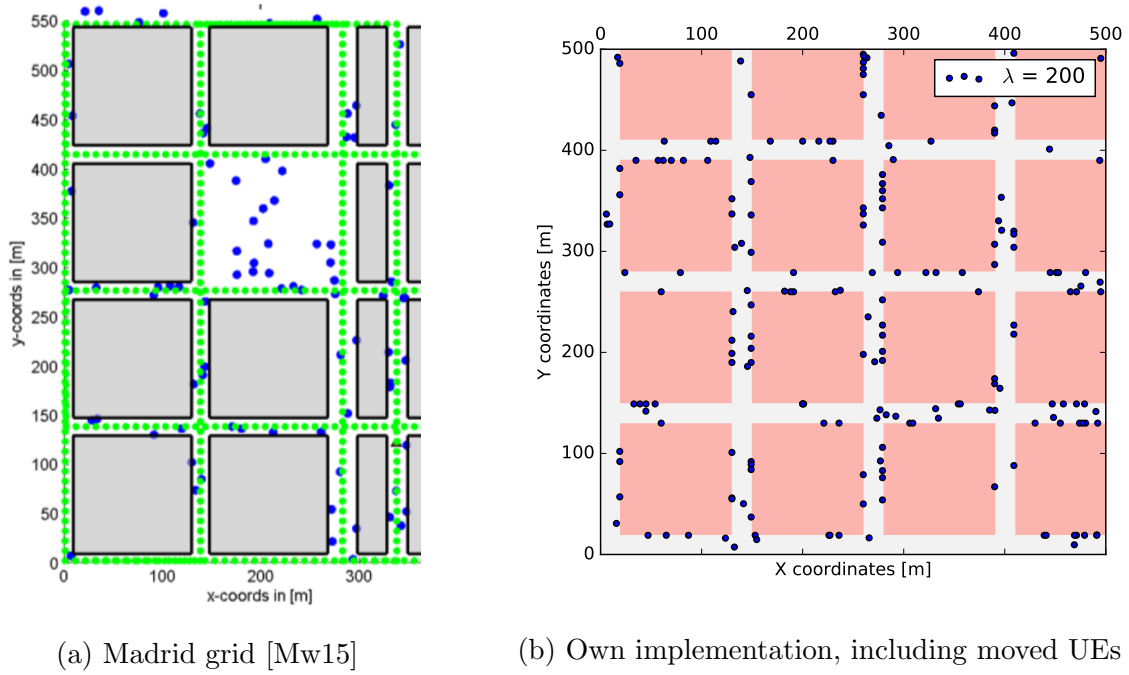


Figure 3.2: Comparison between two Manhattan Grids

The introduction of an explicit grid raises the issue of the positioning of our UEs again. Having scattered them in a Poisson point process (see 3.1), some inevitably now find themselves inside a building and not on the street, as is necessary for our O2O simulations. We overcome this obstacle by simply finding the shortest route from the position inside a block to the street: as the UE position is random, so too is the route taken. Thus we avoid completely discarding the randomness of their positioning. The results can be seen in figure 3.2b and compared to the actual city grid used for METIS measurements (figure 3.2a).

With a Manhattan-like layout at the ready, questions about whether a link has LOS or not become much easier to answer.

### 3.2.2 Line-of-sight

The overall model for pathloss used by [Mw15] is derived specifically from the one presented in [Rep09] by the ITU (International Telecommunication Union) and covers a wide frequency range (0.8 to 60 GHz). Distances between 10 and 500 meters are thus defined by two distinct equations, depending on whether the distance between the two points is greater than a certain “breakpoint distance”. The distance  $d'_{BP}$  in question is defined by

$$d'_{BP} = 0.87 \exp \left( - \frac{\log_{10} \left( \frac{f_c}{1 \text{ GHz}} \right)}{0.65} \right) \frac{4 h'_{BS} h'_{UE}}{\lambda_{WL}}, \quad (3.2)$$

with  $h'_{BS}$  as the effective height of the Base Station and  $h'_{UE}$  the effective height of the UE, with “effective” denoting adjusting for environment height  $h_e$ . The  $\lambda_{WL}$  is the wavelength of the signal, which is calculated from the center frequency  $f_c$  and the speed of light  $c$ . It must be mentioned that for our transmissions, the height of both the origin and destination device will be identical more often than not, due to cluster connections being D2D links.

An additional “pathloss offset”  $PL_1$  is defined in order to bring the model in agreement with the control measurements performed by METIS and is designed to account for elements like multipath fading.

$$PL_{1|dB} = -1.38 \log_{10} \left( \frac{f_c}{1 \text{ GHz}} \right) + 3.34 \quad (3.3)$$

The actual pathloss equations are given as a function of distance  $d$  by

$$PL_{LOS}(d)_{dB} = 10 n_1 \log_{10} \left( \frac{d}{1 \text{ m}} \right) + 28.0 + 20 \log_{10} \left( \frac{f_c}{1 \text{ GHz}} \right) + PL_{1|dB} \quad (3.4)$$

for  $10 \text{ m} < d \leq d'_{BP}$  and

$$PL_{LOS}(d)_{dB} = 10 n_2 \log_{10} \left( \frac{d}{d'_{BP}} \right) + PL_{LOS}(d'_{BP})_{dB} \quad (3.5)$$

for  $d'_{BP} < d \leq 500 \text{ m}$  (compare with [Mw15]). The parameters  $n_1 = 2.2$  and  $n_2 = 4.0$  are the power decay constant on both sides of the break point distance.

### 3.2.3 Non-line-of-sight

Most of the connections available to a given UE will be NLOS links. These happen whenever the UE tries to communicate with a device that is not on its same street and thus the signal has to travel a more convoluted way in order to be received. METIS defers explicitly to the final channel models, created by WINNER+ (Wireless World Initiative

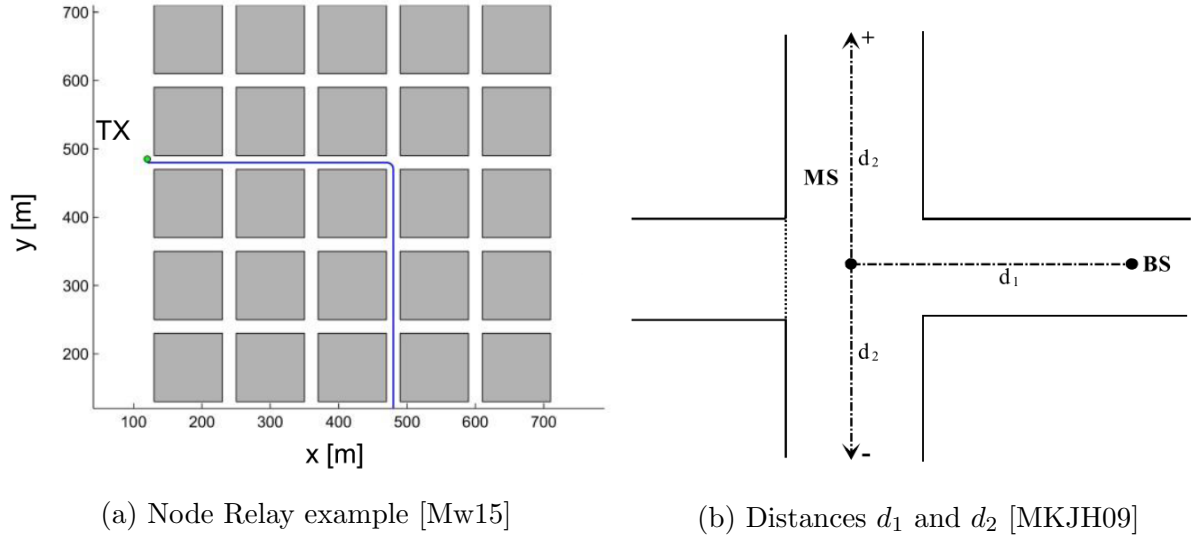


Figure 3.3: Calculation of NLOS path

New Radio+) in [HSK<sup>+</sup>10]. WINNER+ is a private consortium looking to further develop the IMT-A (International Mobile Telecommunications-Advanced) standards.

The conceptual NLOS model in itself comes from an even earlier work, [MKJH09], which details the relevant parameters for NLOS communication in an urban setting. In these cases, the corners resulting from intersecting streets act as relay nodes for the signal. [MKJH09] designates two distances needed to calculate the pathloss in this route, see figure 3.3b, where  $d_1$  is distance from relay node to BS and  $d_2$  to the UE. As was the case for the difference in heights between UE and BS, seeing as the links we are investigating are D2D, there is no real clear theoretical distinction between  $d_1$  and  $d_2$ . However, we keep the distinction intact (with the same emitter/receiver relation) owing to the fact that “[t]hough the pathloss between BS and UE must be the same regardless of the direction of signal transmission due to reciprocity, the pathloss *models* do not necessarily hold the reciprocity” ([Mw15]).

Thus, the formula for pathloss in the studied case is presented in [Mw15] after a small simplification and again featuring the “pathloss offset” (equation 3.3) mentioned in 3.2.2:

$$\begin{aligned}
 PL_{NLOS}(d_1, d_2)_{\text{dB}} = & PL_{LOS}(d_1)_{\text{dB}} + 17.9 - 12.5 n_j \\
 & + 10 n_j \log_{10} \left( \frac{d_2}{1\text{m}} \right) + 3 \log_{10} \left( \frac{f_c}{1\text{GHz}} \right) + PL_{1\text{dB}},
 \end{aligned} \tag{3.6}$$

where  $n_j$  is a power decay constant calculated as

$$n_j = \max(2.8 - 0.0024 d_1, 1.84). \tag{3.7}$$



In a rectangular Manhattan grid such as ours, a only two intersections are needed as relays in order to connect any two given points on the grid. An algorithm was thus created to calculate the shortest possible distance between the two devices using a maximum of two intersections. We take the shortest possible route because the signal spreads omnidirectionally. An example of a calculated route between two points can be seen in figure 3.4.

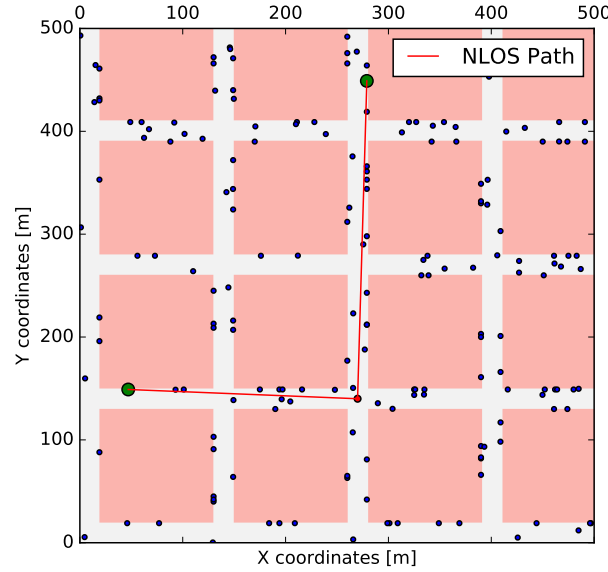


Figure 3.4: Visualization of NLOS path with intersection acting as relay node

### 3.3 Shadow fading

As mentioned in 3.2.1, Shadow Fading - meaning the effects on the signal caused by smaller obstacles - as well as the reflections they create are modelled through a stochastic model. This type of fluctuation, called “Shadow Fading” or “long-term fading” is often realized through a Gaussian distribution in the logarithmic scale (also called a log-normal distribution), as asserted in [FSA04] and shown below in its probability density function. In our case, we followed METIS specifications and set  $\mu_{L_s} = 0$  and  $\sigma_{L_s} = 7\text{dB}$ .

$$p(L_s) = \frac{1}{\sigma_{L_s} \sqrt{2\pi}} \exp\left(-\frac{(L_s - \mu_{L_s})^2}{2\sigma_{L_s}^2}\right) \quad (3.8)$$

While any given point is distributed randomly along the normal distribution, completely random and uncorrelated shadow fading variables make little sense when one considers that the effects of any given set of obstacles won’t change much in the space of a couple

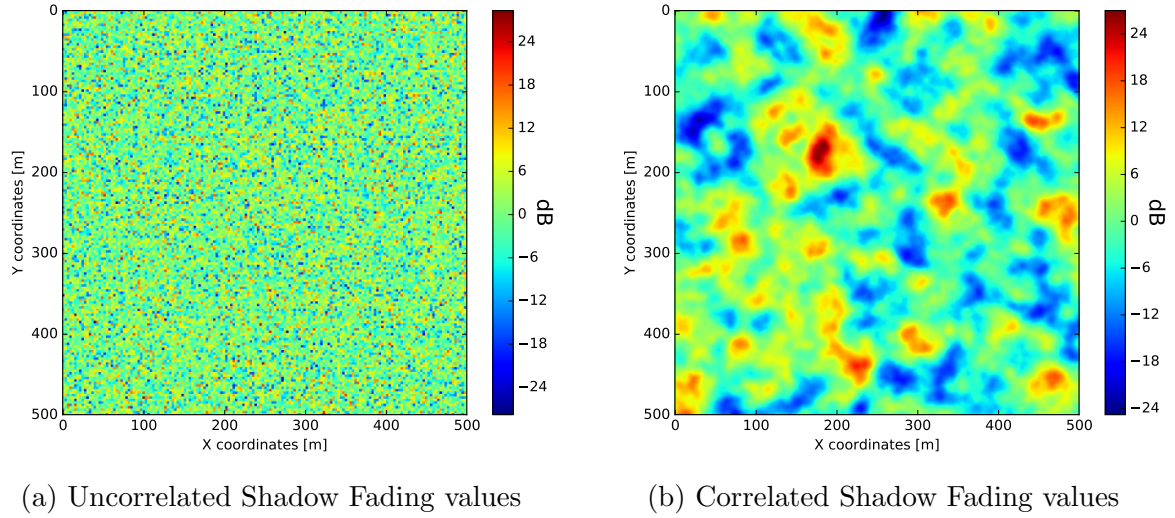


Figure 3.5: Shadow Fading values before and after correlation adjustment

of meters. In order to account for the necessary correlation that these shadow fading variables experience, a normalized autocorrelation function is introduced, both in [FSA04] and [Mw15], with a decorrelation value suggested by METIS  $d_{corr} = 8m$ .

$$R(\Delta x) = \exp \left( - \frac{|\Delta x|}{d_{corr}} \ln(2) \right) \quad (3.9)$$

After generating the shadow fading variables with equation 3.8 and the autocorrelation coefficients with equation 3.9, both matrices are convoluted to generate the correlated values. Convolution does not alter the underlying distribution, but it does elicit a correction of the mean and standard deviation (compare with [FSA04]) in order to return it to the values of the original Gaussian distribution. Our realization is shown below, both before and after the aforementioned correction for spatial correlation.

These shadow fading values are added to the pathloss values in order to fully account for all the obstacles in the way of the signal between two devices. The complete attenuation value then determines the received signal strength at the target device.

A summary of the relevant parameters utilized for the calculation of the pathloss can be seen in table 4.1, part of chapter 4.

### 3.4 Random access procedure and interference

When reducing the load that the eNB experiences as a result of an increase in the amount of devices connecting to it by means of clustering, a large amount of the load is simply

transferred to the cluster heads. These have then to take up the functions of the eNB in terms of implementing a random access procedure through which to service the UEs connecting to it. As mentioned in section 2.2, we contemplate an explicit separation of resources for normal BS to UE communication and D2D communication, putting further constraints on the ability of the cluster head to detect and separate signals using the same resource blocks. In order to best model these kinds of phenomena, the author utilized simulations developed by his supervisor, M.Sc. Mikhail Vilgelm, that were kindly put at his disposition for this work.

Firstly, a Poisson process is used in modeling the arrival of packages proceeding from connected UEs to the appropriate cluster head. This Poisson arrival process is analogous to that shown in equation 3.1 and yields the amount of packages arrived at a certain point in time instead of points in an area. The arrival rate of requests to a given cluster,  $\lambda_A$  was set by recommendation of the author's supervisor to a level where the derivative of the throughput with respect to the arrival rate is positive, at  $\lambda_A = 1.5$ . It is important to note here that the arrival rate is fixed for each cluster head. This means that no matter the amount of UEs connecting to said cluster head, the mean expected amount of requests in a given time frame also remains at a fixed level.

The requests are generated at the given rate and broadcast with a set transmission power  $P_{Tx}$ . Although there are many proposals for power control schemes in D2D communications, such as [EMIA13], [WHS12b] or [LLA15], due to there being so many varied schemes and them adding such complexity to the simulation, it was decided that power control would not be part of the scope of this work. As in [KK14b], we decide to use  $P_{Tx} = 23$  dBm for our simulation, which is incidentally the power level used for coverage issue identification in [3rd12] and the maximum transmit power for public safety defined in [3rd14], both by the 3GPP.

The power is then affected by the appropriate attenuation at the spot of the receiving device (see section 3.2) and the resulting power is the received power  $P_{Rx|dBm} = P_{Tx|dBm} - PL_{dB}$ . In order to assess whether a given signal has reached the cluster head with enough power to be detected, we look at the SINR (Signal-to-Interference-and-Noise-Ratio) of the transmission. For the calculation of the noise we use a thermal noise density  $N_0 = -174 \frac{\text{dBm}}{\text{Hz}}$ , UE receiver noise figure  $NF_{UE} = 9$  dB and system bandwidth  $W = 10$  MHz, as defined in [3rd12], see equation 3.10.

$$P_{N|dBm} = N_0 \cdot W + NF_{dB} \quad (3.10)$$

The incoming requests are checked for additional interference coming from other requests using the same preamble, both within and without the cluster. The received power  $I$  of those interfering signals at the cluster head are added and that total added to the noise power  $P_N$  to finally calculate the SINR, see equation 3.11. As mentioned earlier, the available preambles for transmission of a D2D link are drawn from the overall pool of preambles available in LTE-A. As mentioned in [Cox12], 64 preambles are available to the

cell, only 6 of which are available for D2D communication. This is to allow normal cellular UEs to experience an acceptable QoS (Quality of Service), while still allowing other devices access to the network.

$$SINR = \frac{P_{Rx}}{I + P_N} \quad (3.11)$$

As to the minimum SINR needed to connect to the cluster head, a threshold of  $SINR_{thr} = 10$  dB was chosen within the range presented in [3Gp09] for the minimum ratio necessary to transmit with “an acceptably low BER (Bit Error Rate) in the output data.” Those requests under the threshold will be filtered out before they are dealt with by the cluster head. Please note that although they are not counted towards successful requests, they will count towards interference values of other requests that may or may not clear the threshold.

Finally, requests clearing the threshold will be handled by the cluster head, who will then check for intra-cluster preamble collisions and give feedback, negative or positive, to the UEs. For simplicity’s sake, feedback is assumed to arrive safely back at the UE; positive feedback elicits no action from the original transmitter. Upon reception of negative feedback, on the other hand, the UE “backs off” for an amount of time before attempting the connection once again at a later point in time. If the device is told to back off 20 times, it assumes the connection has failed completely and will not try again until another packet is generated at that UE. The time for each slot was set at 10 ms, while the overall simulation duration was put at 5 s.

Readers can find a summary of all used parameters for this stage on table 4.2, in chapter 4.

The last piece of the puzzle is, of course, the actual mapping of UEs to cluster heads. These are fed into the random access and interference simulation by the clustering algorithms.

### 3.5 Clustering Algorithms

Clustering algorithms determine which UEs will be connected to which cluster heads, as well as which UEs will turn into cluster heads in the first place. Because of the nature of our research (regarding D2D communication), we eschewed any schemes that required dedicated gateways into the networks. In the definition of the scope of this work, we also decided to leave out any algorithms with multi-hop possibilities, simply due to the sheer complexity that would have represented. Algorithms presented here thus feature only one aggregation stage at the cluster head, which then forwards the data to the eNB.

Most of the work done in clustering algorithms for wireless networks comes from the area of Wireless Sensor Networks (WSN), where large amounts of sensor nodes form a network

communicating with a central unit of control. These types of structures lend themselves especially to grouping and aggregation, considering especially that there is often a lot of redundancy in the collected data. Energy efficiency and resilience of networks is often of paramount importance, in an attempt to minimize maintenance overhead. There have been several studies about clustering algorithms in this area, such as [JYZ09] or [ATN14]. Unfortunately, the fundamentally different nature between static sensors and LTE-A capable devices severely limits the applicability of most schemes to our scenario.

Additionally to a WSN algorithm we included schemes normally used in statistical data analysis, specifically a couple of hierarchical clustering schemes. These feature a progressive merging of clusters depending on a variety of criteria; distance is often used when determining the level of kinship two points or clusters possess. Hierarchical clustering is preferred over other types of schemes due to us working under the assumption that there is few information present in the system a priori. This assumption makes the necessary estimation of the final number of clusters (cf. [ELLS11]) exceedingly complicated; implementing advanced heuristics or other such techniques to overcome this was of no interest to us.

When possible, we have tried instead to use measures relevant to our research area, such as Signal-to-Noise Ratio (SNR) and Signal-to-Interference-and-Noise Ratio (SINR) to quantify connectivity.

### 3.5.1 LEACH

One of the most influential clustering algorithms in WSNs is LEACH (Low-Energy Adaptive Clustering Hierarchy), presented in [HCB00]. Despite its relative age, it promised “localized coordination to enable scalability and robustness for dynamic networks” and was designed to lower the amount of information transmitted to the base station. As can be seen in [ATN14], it has spawned many other algorithms based on its simple premises.

LEACH works by randomly assigning its nodes as cluster heads according to a certain formula intended to yield a desired percentage  $P_{LEACH}$  of CHs. Each node generates a uniformly distributed number between 0 and 1 and compares it to a threshold value  $T(n)$ . If the generated number is over that threshold it is designated to function as a cluster head.

Once cluster heads have been assigned for the whole of the network, an advertisement is broadcast, announcing to the other UEs which cluster heads are available. UEs then take the received signal strength as a proxy for distance and elect the nearest to their location. We simulate this behavior by creating a link to the received signal with the highest SNR. Signal must exceed an SNR of 0 to even be considered for a potential link, in order to ensure the advertisement is distinguishable from the noise.

LEACH is designed to work with several rounds of CH assignment and data transfer in

order to rotate the burden of CH selection, assuming a fixed set of nodes for a relatively long period of time. Seeing how our scenario is short-lived and features ideally mobile nodes, as well as a highly mutable network layout, we eschew the round structure. Consequently, the resulting formula for the generation of the threshold value  $T(n)$  can be seen in equation 3.12

$$T(n) = \frac{P_{LEACH}}{1 - P_{LEACH} \pmod{\frac{1}{P_{LEACH}}}} \quad (3.12)$$

Having observed just how many other clustering schemes it inspired, we decided to give LEACH particular importance in our testing, running simulations for it with a wider range of point densities  $\lambda$ , as well as more fine-grained data points.

### 3.5.2 Complete-Link Clustering

Also known as “farthest neighbor clustering”, Complete-Linkage Clustering “[t]ends to find compact clusters with equal diameters” ([ELLS11]). It does so by defining the distance between two clusters as the maximum distance between their members, see equation 3.13, from [Sha09].

$$d(A, B) = \max_{\vec{x} \in A, \vec{y} \in B} \|\vec{x} - \vec{y}\| \quad (3.13)$$

Instead of using euclidean distance, as is the norm, we instead define the distance between two points as the SNR between them. Note that this “reverses” the algorithm’s logic, meaning that instead of finding the minimum distance among all maximum distances in a cluster for a merge, we find the maximum SNR among all minimum SNRs inside a cluster. The algorithm then takes two clusters with the smallest such SNR “distance” and merges them. Normally, it would continue to do so until there are no more clusters to merge, i.e. there only remains one cluster containing all the points in the set. In order to avoid this, with every potential merge of two clusters, we check if the potential D2D link is over a certain threshold. For this threshold we chose the same threshold introduced in section 3.4, 10dB. When no further links under that level are possible, the algorithms stops. The fact that we are using only single-hop aggregation constrains our options quite starkly; a viable link must be possible to all members of the cluster.

In this type of scheme, the election of the cluster head seems almost arbitrary. In order to maintain verisimilitude of the simulation, we designate the UE with the smallest average distance to all other UEs as the cluster head.

### 3.5.3 Single-Link Clustering

The “nearest neighbor technique”, second of the best-known hierarchical algorithms and “one of the simplest hierarchical clustering methods” ([ELLS11]) defines the distance between two clusters as “the minimum distance between their members”, see equation 3.14. This means that only one link will define the proximity between two entities, regardless of the density of the points inside them.

$$d(A, B) = \min_{\vec{x} \in A, \vec{y} \in B} \|\vec{x} - \vec{y}\| \quad (3.14)$$

Here, too, we redefine the distance between two points as the SNR between the two. Despite its similarity to Complete-Link (see above, section 3.5.2), the nature of the algorithm makes it “[not] care about compactness or balance” [Sha09]. Preliminary tests showed that setting the same criteria for stopping as in Complete-Link would result most often in a gigantic, all-encompassing cluster containing all UEs, completely negating the effect of data aggregation.

Consequently, we defined a stopping criteria not based on a threshold  $SNR$ , but rather on a threshold percentage of UEs serving as clusters  $P_{SINGLE}$ , analogous to the  $P_{LEACH}$  of LEACH. The resulting number of clusters is then defined as

$$\text{Desired number of clusters} = P_{SINGLE} \cdot \lambda. \quad (3.15)$$

The values chosen for  $P_{SINGLE}$  cover the same range as those of  $P_{LEACH}$ . This adjustment makes comparison with the other clustering algorithms significantly easier and allows us to still use Single-Link as an algorithm. Here, just as in Complete-Link, we define the cluster head as the UE with the lowest average distance to all other UEs.

### 3.5.4 Ward’s Method

Originally formulated as an approach in 1963, in [War63], Ward’s method provides an interesting cost metric for the merging of two clusters. As stated more succinctly in [Sha09], the method “says that the distance between two clusters, A and B, is how much the sum of squares will increase when we merge them”. Ward formulates a merging cost  $\Delta(A, B)$  based on the the distance between the geographical center of each cluster and utilizes this information to merge the two clusters with the lowest cost:

$$\Delta(A, B) = \frac{n_A n_B}{n_A + n_B} \|\vec{m}_A - \vec{m}_B\|^2, \quad (3.16)$$

with  $n_A$  and  $n_B$  the number of points in the cluster and  $\vec{m}_A$  and  $\vec{m}_B$  the center of clusters A and B. The “center” of the cluster in our own implementation remains the geographical center.

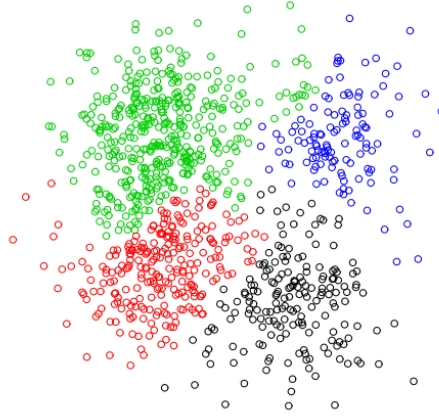


Figure 3.6: Sample clustering as a result of Ward's Method [Sha09]

Here again, a limit must be provided for the algorithm not to form a single gigantic cluster; we continue using the D2D communication threshold 10dB. When the algorithm detects that there are no further connections possible over the given limit, it stops. A simple implementation of the algorithm can be observed in figure 3.6.

The assignment of the cluster head occurs as in both of the other hierarchical algorithms.



# Chapter 4

## Results

### 4.1 Evaluation methodology

In this chapter, we will be presenting and evaluating the results yielded by our simulation. As stated in more detail in chapter 3, the scenario that we are implementing here is that of a highly dense urban environment. Points are distributed according to a homogeneous PPP (section 3.1) in a set Manhattan grid (3.2.1). Pathloss between two points accounts for both the topology of the grid as well as spatially-correlated shadow fading (3.3). Clusters are created according to the specifications of various clustering schemes (3.5) and then the resulting traffic is simulated with a random access procedure at the assigned cluster heads (3.4), where both noise and interference are accounted for.

All parameters utilized in our simulation are gathered in the two tables below, separated into those relevant for the calculation of pathloss (table 4.1) and those relevant for random access and interference simulation (table 4.2).

The central element that testing will be looking at is how the chosen clustering algorithms behave under varying degrees of mean UE density  $\lambda$ . In the case of LEACH, due to CH selection probability  $P_{LEACH}$  also being a relevant parameter, we will also test for a range of values.

Regarding the metrics used for comparison of adequacy of the different clustering schemes, we managed to narrow them down to four criteria:

- Percentage of UEs connecting to eNB
- Mean channel utilization rate
- Total resource efficiency
- Mean UE drop ratio

Parameter	Value
<b>PPP</b>	
Mean point density $\lambda$ (range)	50 – 1000
<b>Pathloss</b>	
Center Frequency $f_c$	2 GHz
Wavelength $\lambda_{WL}$	0.15 m
Speed of light $c$	$3 \cdot 10^8 \frac{\text{m}}{\text{s}}$
Height of UE $h_{UE}$	1.5 m
Height of BS $h_{BS}$	10 m
Environment height $h_e$	1 m
Power decay constant $n_1$	2.2 dB
Power decay constant $n_2$	4.0 dB
<b>Shadow Fading</b>	
Shadow Fading mean $\mu_{L_s}$	0 dB
Shadow Fading standard deviation $\sigma_{L_s}$	7 dB
Decorrelation distance $d_{corr}$	8 m

Table 4.1: Parameters relevant for pathloss calculation

Parameter	Value
<b>Request creation &amp; transmission</b>	
Request arrival rate $\lambda_A$	1.5
Maximum connection attempts	20
Transmission power $P_{Tx}$	23 dBm
<b>Noise</b>	
Noise density $N_0$	$-174 \frac{\text{dBm}}{\text{Hz}}$
UE receiver noise figure $NF_{UE}$	9 dB
BS receiver noise figure $NF_{BS}$	5 dB
System Bandwidth $W$	10 MHz
<b>Interference</b>	
Number of total LTE-A preambles	64
Number of preambles available for D2D communication $m$	6
SINR threshold $SINR_{thr}$	10 dB
Slot duration $T_{slot}$	10 ms
Total duration $T_{total}$	5 s

Table 4.2: Parameters relevant for random access and interference

In the following, we will shortly justify and explain each metric.

#### 4.1.1 Percentage of UEs connecting to eNB

One of the original motivations behind the expansion of LTE-A through D2D proximity services is the alleviation of the load experienced by the available infrastructure with large numbers of devices. By measuring the percentage of UEs connecting directly to the eNB, we seek to quantify to what extent the given algorithm is actually reducing the traffic at the eNB.

We denote as  $P_{UE \rightarrow eNB}$  and define it as

$$P_{UE \rightarrow eNB} = \frac{\text{UEs without cluster assignment}}{\text{Total UEs in grid}}, \quad (4.1)$$

with UEs without cluster assignment meaning those that are neither transmitting to a cluster head nor are one themselves.

It is important to note here that this measure, as with all presented in this work, is not unambiguous. A very small  $P_{UE \rightarrow eNB}$  may look good from the point of view of the amount of connections at the eNB, but it may belie overly large clusters that only transfer the overload problem from the base station to the individual cluster heads.

#### 4.1.2 Mean channel utilization rate

Throughput is often used in communication networks as a measure of the amount of data being transmitted in a given time frame. In a similar vein, our measure of mean channel utilization rate, measured at individual cluster heads and then averaged over them, intends to quantify to what extent the available channel is being utilized to its full potential.

The definition given here for mean channel utilization rate  $\varrho$  was proposed by this work's supervisor and is defined as

$$\varrho_{channel} = \frac{N_{successes}}{m \cdot N_{slots}}, \quad (4.2)$$

with  $N_{successes}$  being the amount of successful connections that have been established with the cluster head,  $m$  the number of preambles available for transmission (cf. section 3.4) and  $N_{slots}$  the number of available time slots for transmission (see equation 4.3).

$$N_{slots} = \frac{T_{total}}{T_{slot}} - 1 \quad (4.3)$$

The final mean channel utilization rate  $\bar{\varrho}_{channel}$  is then averaged out over all cluster heads.

It is worth noting how remarkably small the resulting values are for  $\bar{\varrho}_{channel}$  across all measurements: this is mostly due to the way we defined the metric in the first place. Firstly, the fixed arrival rate of requests to the CH,  $\lambda_A$  is kept constant at a low value of 1.5, which automatically lowers the amount of *successful* requests  $N_{successes}$ . This is of course compounded by the fact that, with a  $T_{total} = 5$  s and a  $T_{slot} = 0.01$  s,  $N_{slots}$  evaluates to 500.

### 4.1.3 Total resource efficiency

The inclusion of resource efficiency as a metric was born out of a desire to have a measure that somewhat quantified the potential gains that the expansion of LTE-A into D2D communication can have. To this effect, we looked into the work presented in [KK14a], where it is sought to introduce a measure for efficiency in D2D communications. The authors, recognizing how traditional measures such as throughput, do not accurately reflect the gains of D2D, propose a measure of resource efficiency for the whole network  $RE(\mathcal{G})$  based on the available resources it uses:

$$RE(\mathcal{G}) = \sum_{w_{ij} \in \mathcal{W}} \eta_{ij} RE(w_{ij}). \quad (4.4)$$

In the above equation,  $\eta_{ij}$  is the fraction of resources  $r(w_{ij})$  used out of the total resource pool  $\mathcal{R}(\mathcal{G})$  by a link  $w_{ij}$  out of all links  $\mathcal{W}$

$$\eta_{ij} = \frac{|r(w_{ij})|}{|\mathcal{R}(\mathcal{G})|} \quad (4.5)$$

and  $RE(w_{ij})$  is the efficiency of the individual link  $w_{ij}$

$$RE(w_{ij}) = \frac{TP(w_{ij}) \cdot T_{total}}{|r(w_{ij})|}, \quad (4.6)$$

measured with help of the link throughput  $TP(w_{ij})$ , the total observed time length  $T_{total}$  (cf. section 3.4). Total resource efficiency given in  $\frac{\text{bit}}{\text{s} \cdot \text{Hz}}$ .

The total resource pool  $\mathcal{R}(\mathcal{G})$  we define, similarly to [KK14a] as the Cartesian product  $\mathcal{R} = \mathcal{T} \times \mathcal{F}$  of available time ( $\mathcal{T}$ ) and frequency ( $\mathcal{F}$ ) resources. We eschew a definition of available area resources  $\mathcal{A}$  due to the difficulty of defining them in this context, an issue acknowledged by the authors, who also exclude it in their examples.

### 4.1.4 Mean UE drop ratio

Finally, we include a measure to quantify how successful a given device is in transmitting the information it has to. To do this, we look at the amount of times it “is dropped” by its

respective cluster head, meaning all the times the “back off” limit is reached (see section 3.4). We then compare it to all attempts, both failures and successes:

$$\theta_{drops} = \frac{\text{Number of Failures}}{\text{Number of Successes} + \text{Number of Failures}}. \quad (4.7)$$

We then average this across all UEs communicating through D2D to find the final mean UE drop ratio  $\bar{\theta}_{drops}$ .

## 4.2 LEACH

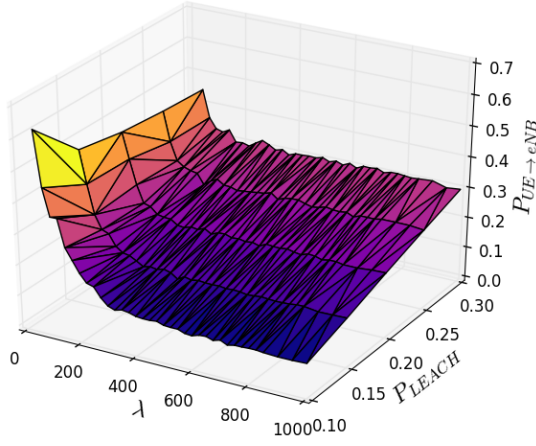
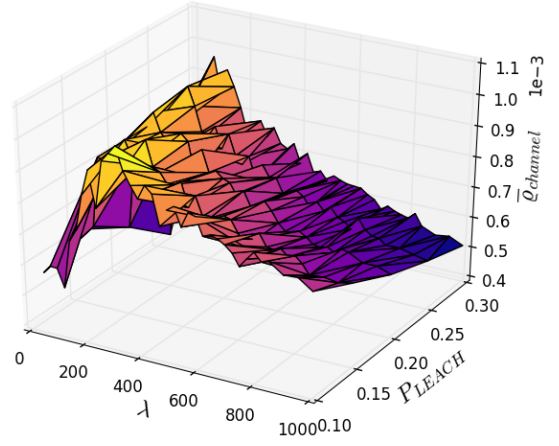
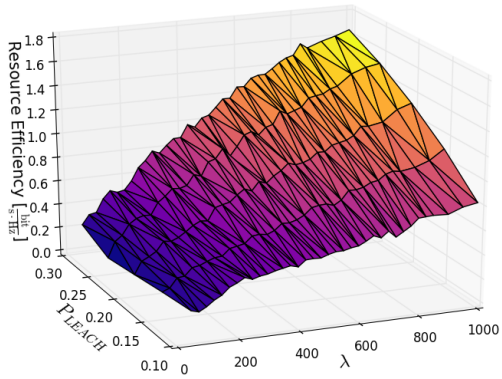
As stated in the previous chapter, LEACH was of particular interest to us due to the influence it had had on so many other clustering algorithms in the field of WSNs (see section 3.5.1), as well as the simplicity it presented. The presence of not only the expected point density  $\lambda$  but also the cluster head activation probability  $P_{LEACH}$  raised many questions about how the network would react to changes in both. We accordingly expanded the range of  $\lambda$  of our simulation from the usual  $[50 - 500]$  to  $[50 - 1000]$ . The overall results can be appreciated in figure 4.1. In the following, all figures are presented with a confidence interval, when existing, of 85%.

Regarding the **percentage of UEs connecting to eNB**  $P_{UE \rightarrow eNB}$  (figure 4.2), after an initial sharp increase, it goes down steadily, leveling out starting around the  $\lambda = 400$  mark (see figure 4.2). This “final” value is closely correlated to the cluster head activation probability  $P_{LEACH}$ : for  $P_{LEACH} = 0.1$ ,  $P_{UE \rightarrow eNB}$  saturates around the 10% mark, for  $P_{LEACH} = 0.3$ ,  $P_{UE \rightarrow eNB}$  it moves towards 30%, etc.

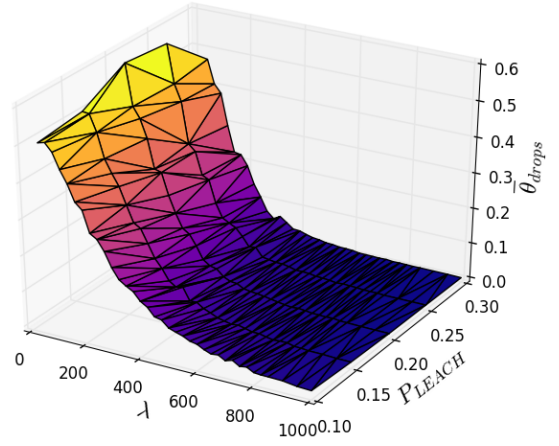
This is of course, expected behavior. The initial increase in  $P_{UE \rightarrow eNB}$  can be explained by insufficient device density: having no viable cluster heads around them, devices elect to transmit their data through other means and not through D2D. Once a high enough concentration of UEs, and consequently of cluster heads is available, most UEs are able to connect to a cluster head in their vicinity. The only UEs left to transmit directly to the eNB are, of course, the cluster heads themselves.

It should be noted that  $P_{UE \rightarrow eNB}$  is a *percentage* and scales with absolute numbers. while 10% seems like a small value, with a mean point density of, say, 700, it means around 70 devices trying to gain access the eNB’s resources. Even after data aggregation, a very high  $\lambda$  means placing an inordinate amount of pressure on the available PUSCH resources.

Observing the **mean channel utilization rate**  $\bar{\varrho}_{channel}$  (figure 4.3) is, unfortunately, not as straightforward. Despite the interesting shapes promised in figure 4.1b, the high variance present in the data and visualized in figure 4.3 makes it impossible to take it too seriously. Despite this,  $\bar{\varrho}_{channel}$  seems to experience a worsening behavior as  $\lambda$  increases. Like  $P_{UE \rightarrow eNB}$ , it also experiences its lowest values with low device densities.

(a) % of UEs connecting to eNB  $P_{UE \rightarrow eNB}$ (b) Mean channel utilization rate  $\bar{\rho}_{channel}$ 

(c) Total resource efficiency

(d) Mean UE drop ratio  $\bar{\theta}_{drops}$ Figure 4.1: Behavior of LEACH compared to  $P_{LEACH}$  and  $\lambda$

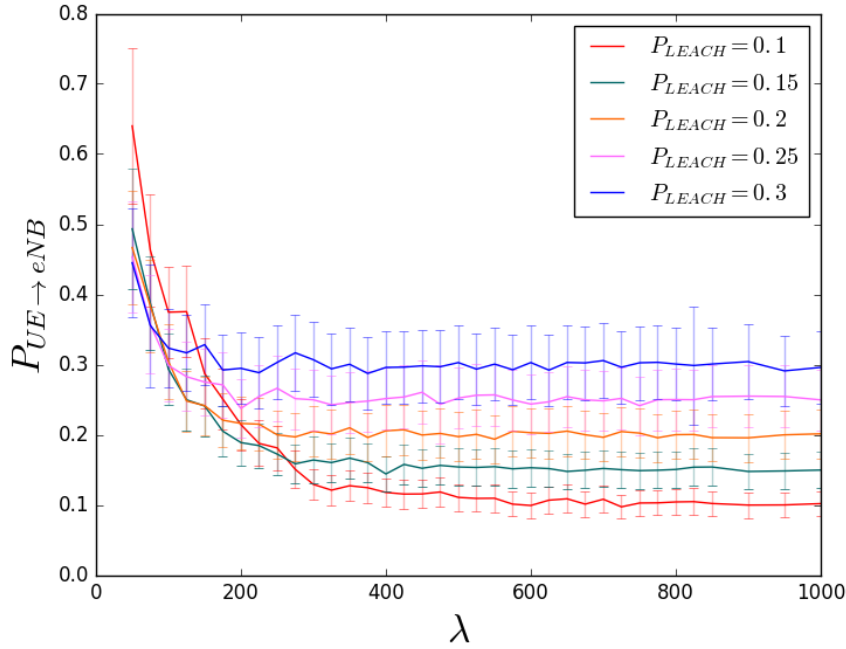


Figure 4.2: LEACH: Percentage of UEs connecting to eNB  $P_{UE \rightarrow eNB}$  in relation to mean point density  $\lambda$

We also consider this to be expected behavior: with very small, very ineffective clusters at low densities, the available resources are severely underutilized: clusters cannot be formed efficiently and the individual devices connect directly to the eNB. Towards higher values, it exhibits the contrary situation; very high densities mean a very high amount of available cluster heads and smaller clusters when compared to middling values of  $\lambda$ , making the average utilization go down, since each cluster serves fewer UEs. The highest value of  $\bar{\varrho}_{channel}$  is thus achieved with a low CH activation probability  $P_{LEACH} = 0.1$  and a middling  $\lambda = 325$ .

Moving on to **total resource efficiency** (figure 4.4), the data seems pretty straightforward. Total resource efficiency increases with both mean point density  $\lambda$  and cluster head activation probability  $P_{LEACH}$ . With more viable D2D connections, more devices are sharing the same pool of resources, both in time and frequency, as is explained in 4.1.3.

While this seems to bode well for very dense networks, it is important to point out that this behavior can also be in part explained with the increase in brute D2D connection numbers that occurs with increasing values of the two variables. A more accurate measure would have to take into account the connection to the eNB with more detail, as well as the higher amount of interference caused. As mentioned earlier, this is also compounded with a mounting pressure on the resources of the eNB, which may not be able to handle both the high  $\lambda$  and high resource efficiency that a simple optimization towards this measure would suggest.

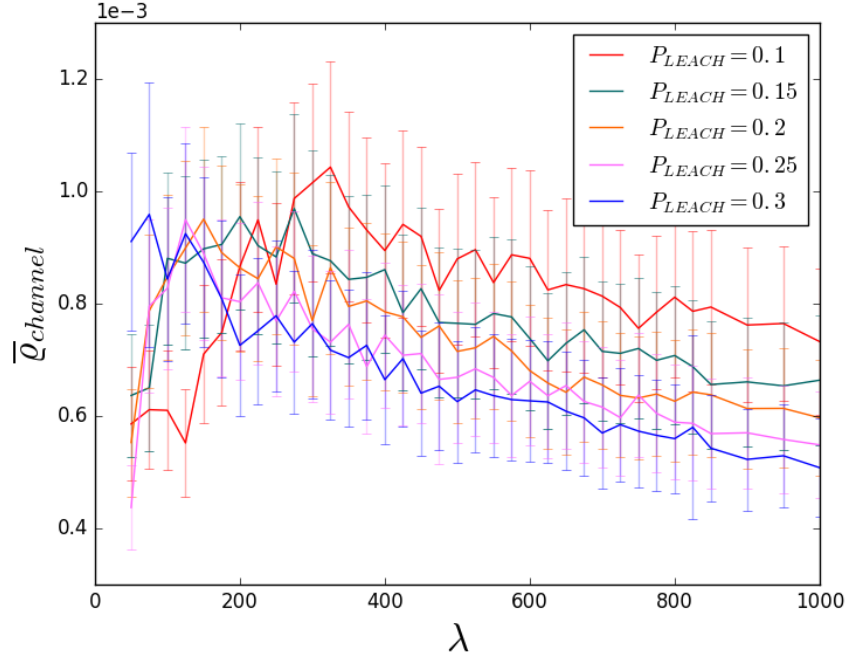


Figure 4.3: LEACH: Mean channel utilization rate  $\bar{Q}_{channel}$  in relation to mean point density  $\lambda$

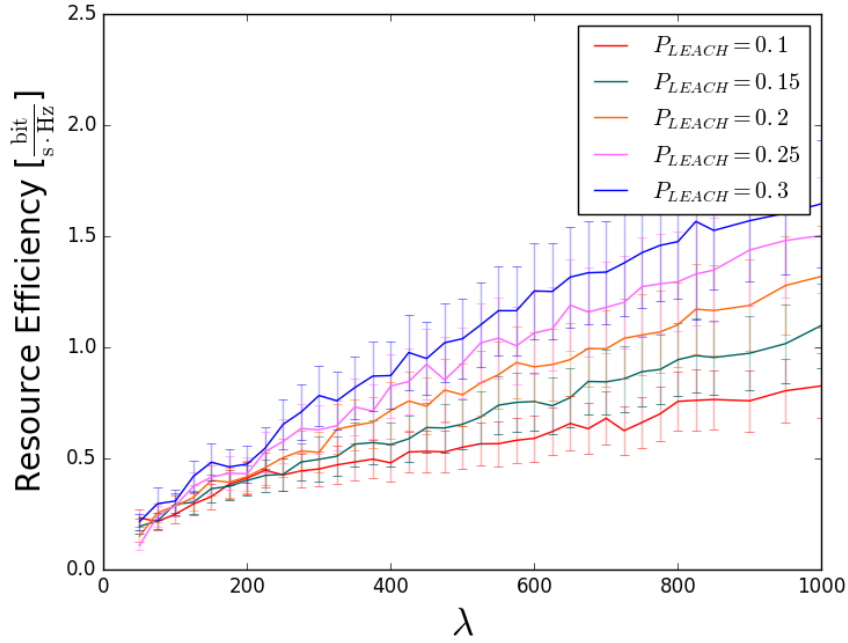


Figure 4.4: LEACH: Total resource efficiency in relation to mean point density  $\lambda$



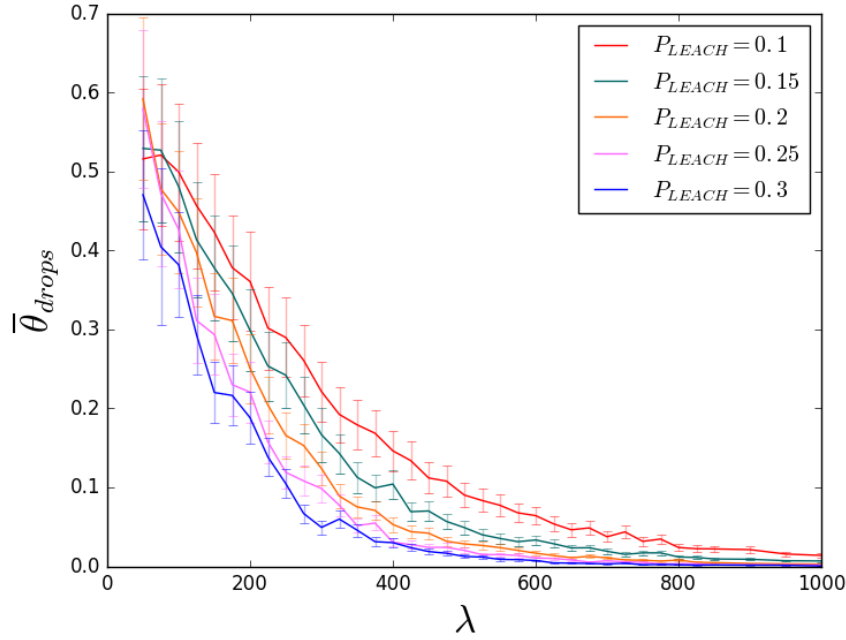
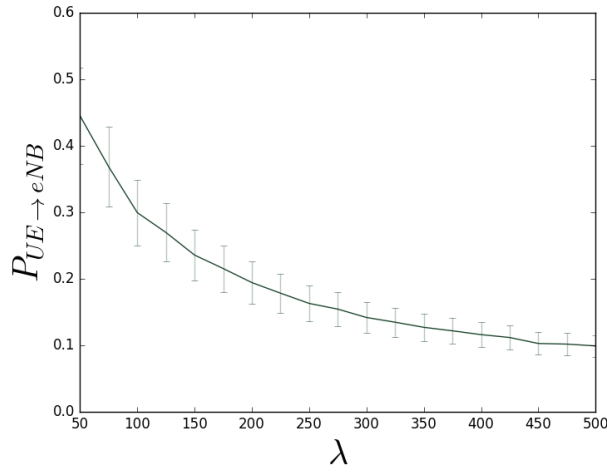
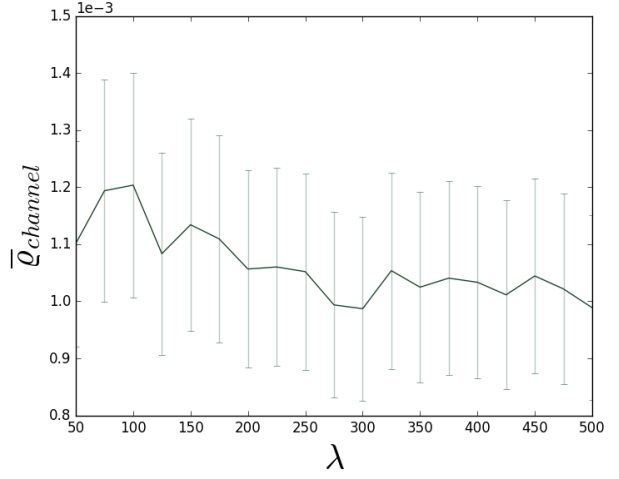
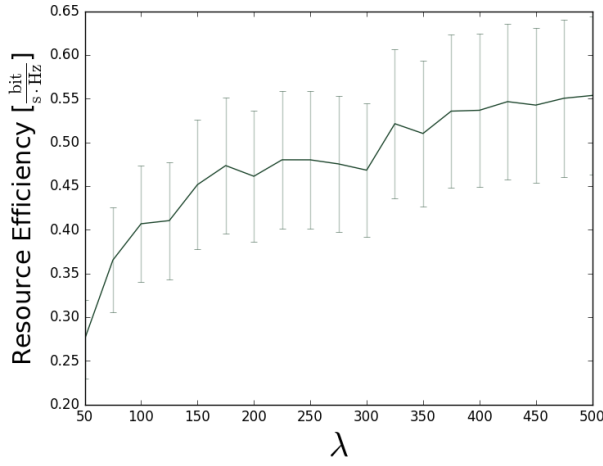


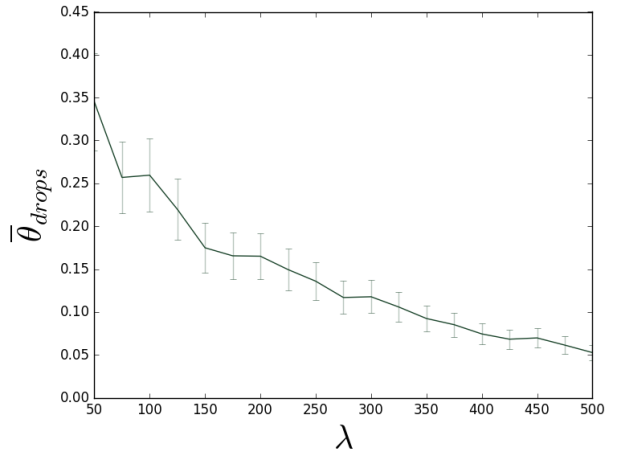
Figure 4.5: LEACH: Mean UE drop ratio  $\bar{\theta}_{drops}$  in relation to mean point density  $\lambda$

Finally, we regard **mean UE drop ratio**  $\bar{\theta}_{drops}$  (figure 4.5). Here, all curves present a downward trend with an increasing  $\lambda$ , with higher values of  $P_{LEACH}$  presenting lower ones of  $\bar{\theta}_{drops}$ . With increasing density of devices, as well as density of cluster heads, the amount of times a UE is completely unsuccessful at connecting after 20 “back offs” falls to nearly 0.

Intuitively, one might expect that  $\bar{\theta}_{drops}$  would steadily rise after a period of falling, reacting to the increased interference that is caused by a large amount of devices interfering all at the same time. The explanation for this, lies again in the arrival rate of requests at the cluster head  $\lambda_A$ . As explained in section 3.4, the arrival rate remains constant, irrespective of the amount of UEs connected to a cluster head. An increase in density  $\lambda$ , which would often result in an increase in the number of devices connected thus does *not* in fact cause an increase in the amount of requests. On the contrary, the amount of requests coming from a given UE in any time frame goes down when the size of its cluster grows. The negative effects of interference, though taken well into consideration, become negligible with such sparse rates of communication.

(a) % of UEs connecting to eNB  $P_{UE \rightarrow eNB}$ (b) Mean channel utilization rate  $\bar{\varrho}_{channel}$ 

(c) Total resource efficiency

(d) Mean UE drop ratio  $\bar{\theta}_{drops}$ Figure 4.6: Behavior of Complete-Link clustering compared to  $\lambda$

## 4.3 Hierarchical Algorithms

### 4.3.1 Complete-Link

In figure 4.6a concerning **percentage of UEs connecting to eNB**  $P_{UE \rightarrow eNB}$ , we see a steady lowering of  $P_{UE \rightarrow eNB}$  towards a saturation value of around 0.1. Unlike LEACH or Single-Link, this value is “organic”, since the stopping criteria for the algorithm is purely the SNR threshold previously defined.

**Mean channel utilization rate**  $\bar{\rho}_{channel}$  (figure 4.6b) shows an even weaker trend downwards than is the case in LEACH, although the high variance in the data once again restricts conclusive observations in this area. It is fair to say, however, that there does not seem to exist a strong correlation between  $\lambda$  and  $\bar{\rho}_{channel}$  in this clustering scheme.

**Total resource efficiency**, in figure 4.6c, experiences a stronger upswing on the lower end of the  $\lambda$  axis and continues to grow throughout, albeit in a more tentative manner. The magnitude of the values stays within a similar range as LEACH, as will be further explored in section 4.4.

Lastly, the **mean UE drop ratio**  $\bar{\theta}_{drops}$  plotted in figure 4.6d shows an overall downward trend, as was expected from our other simulations.

### 4.3.2 Single-Link

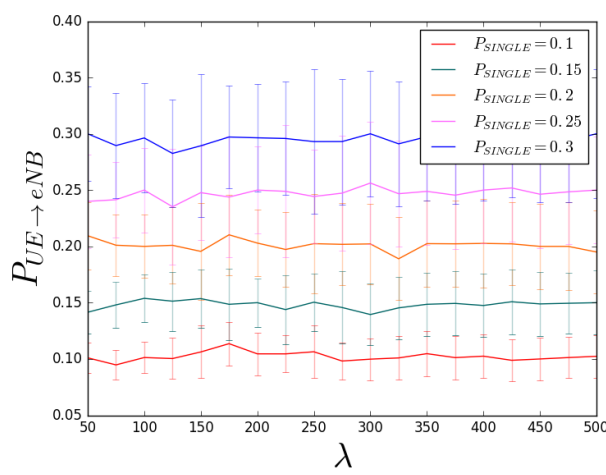
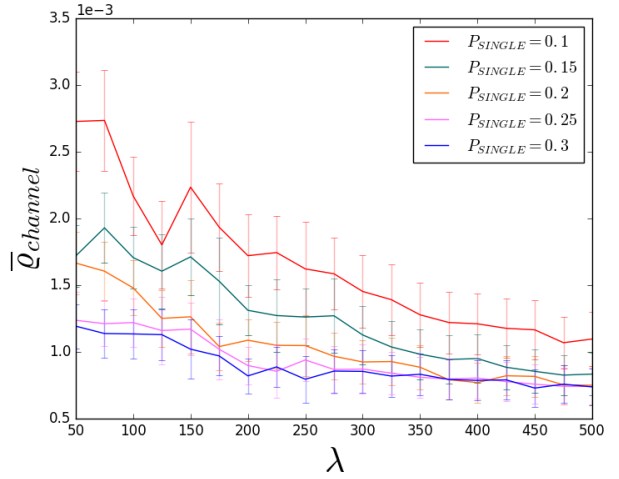
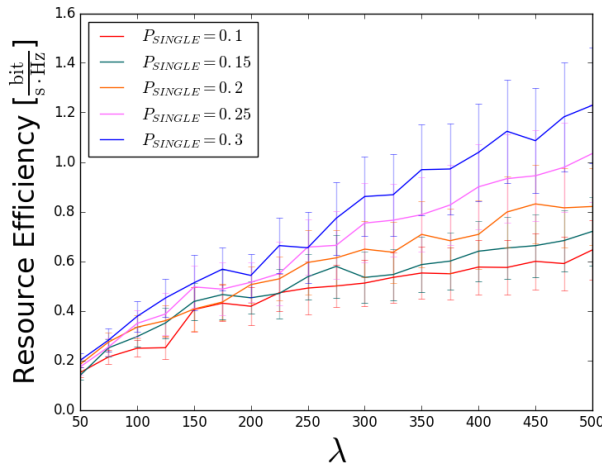
For Single-Link, we took a similar approach to that of LEACH, owing to the stark similarities between the two. As discussed in 3.5.3, we used the same values for  $P_{LEACH}$  and  $P_{SINGLE}$ , both to highlight the similarities and better tease apart the differences.

It makes little sense to discuss the plot featured in figure 4.7a detailing the **percentage of UEs connecting to eNB**  $P_{UE \rightarrow eNB}$ . Due to the very definition of  $P_{SINGLE}$  in section 3.5.3, it's clear that  $P_{UE \rightarrow eNB}$  will remain at roughly the same level throughout all levels of  $\lambda$ . The fluctuations are only due to the variance of the Poisson process used to generate the positions of our UEs.

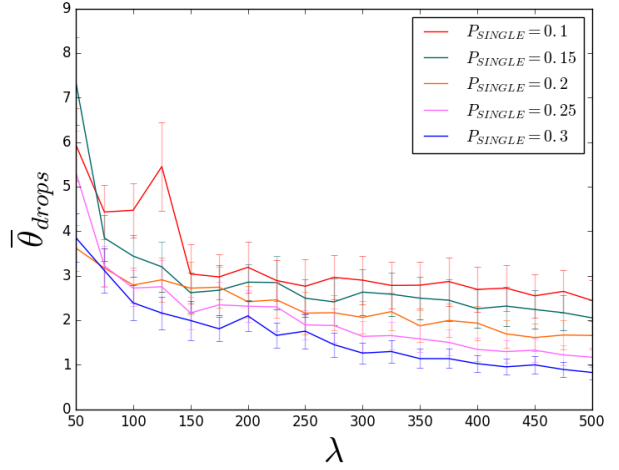
Regarding figure 4.7b and the **mean channel utilization rate**  $\bar{\rho}_{channel}$ , it seems noteworthy that the variance for the metric is not as disruptive as that of earlier observations. The downward trend is clear and, as with LEACH, higher CH density roughly correlates with lower  $\bar{\rho}_{channel}$ , although in this case the relationship is maintained even in lower values of  $\lambda$ .

**Total resource efficiency** (figure 4.7c) also exhibits a remarkably close behavior to that of LEACH. We will compare them directly in section 4.4 to disentangle the differences between both.

The **mean UE drop ratio**  $\bar{\theta}_{drops}$  plots of figure 4.7d TERMINAR

(a) % of UEs connecting to eNB  $P_{UE \rightarrow eNB}$ (b) Mean channel utilization rate  $\bar{Q}_{channel}$ 

(c) Total resource efficiency

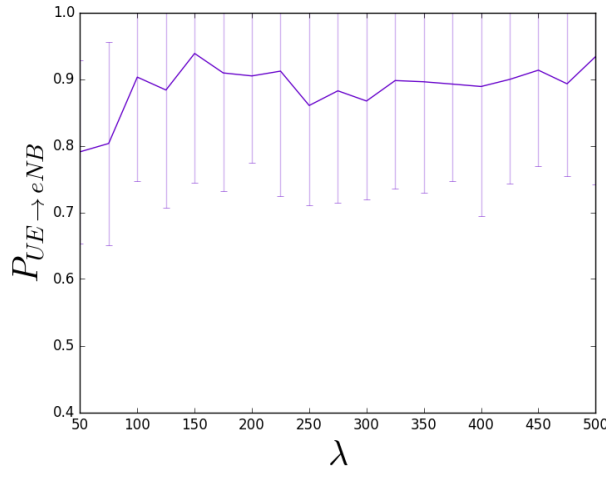
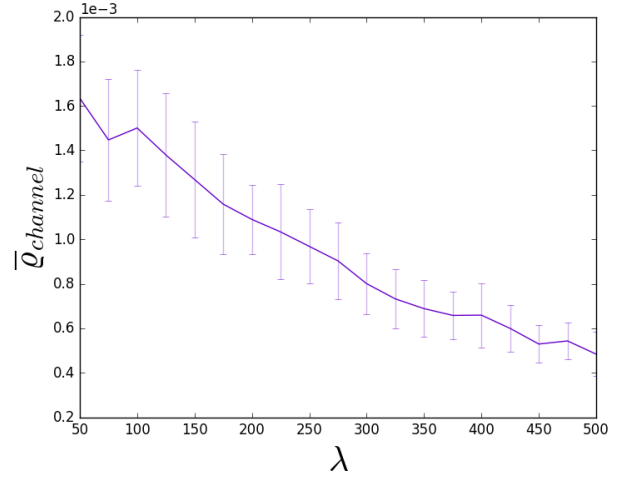
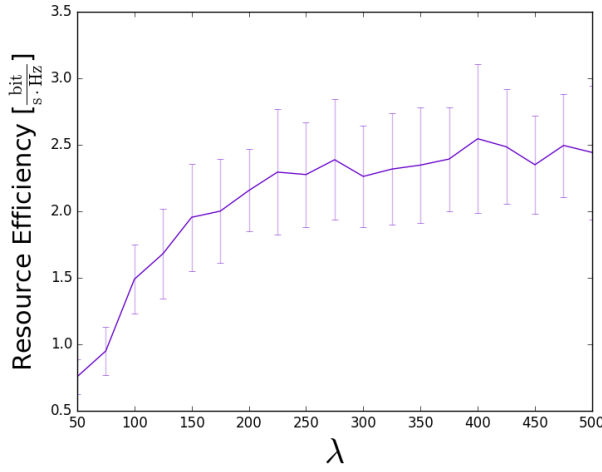
(d) Mean UE drop ratio  $\bar{\theta}_{drops}$ Figure 4.7: Behavior of Single-Link clustering compared to  $\lambda$

### 4.3.3 Ward's Method

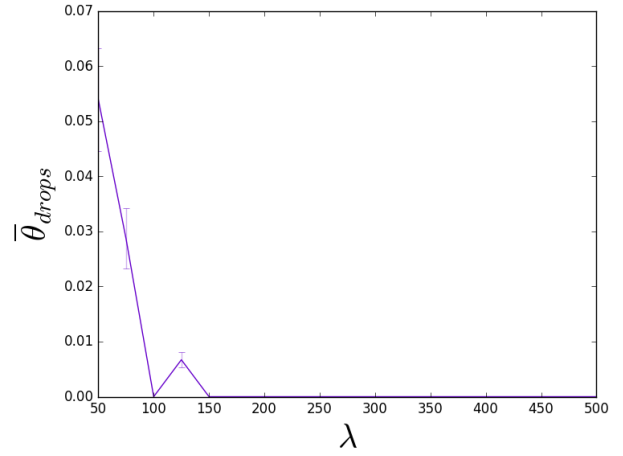
Looking at the results given by Ward's method, it is immediately apparent that this was the worst clustering scheme, in terms of actually managing to provide structures to alleviate the pressure on the eNB's resources. This observation is easily explained by simply glancing at figure 4.8a, where  $P_{UE \rightarrow eNB}$  is detailed. The metric hovers constantly around 90%, meaning that the large majority of UEs are unable to be grouped into a viable cluster and elect to transmit their information through traditional means. This rate is simply unacceptable for highly dense applications like the one we are investigating.

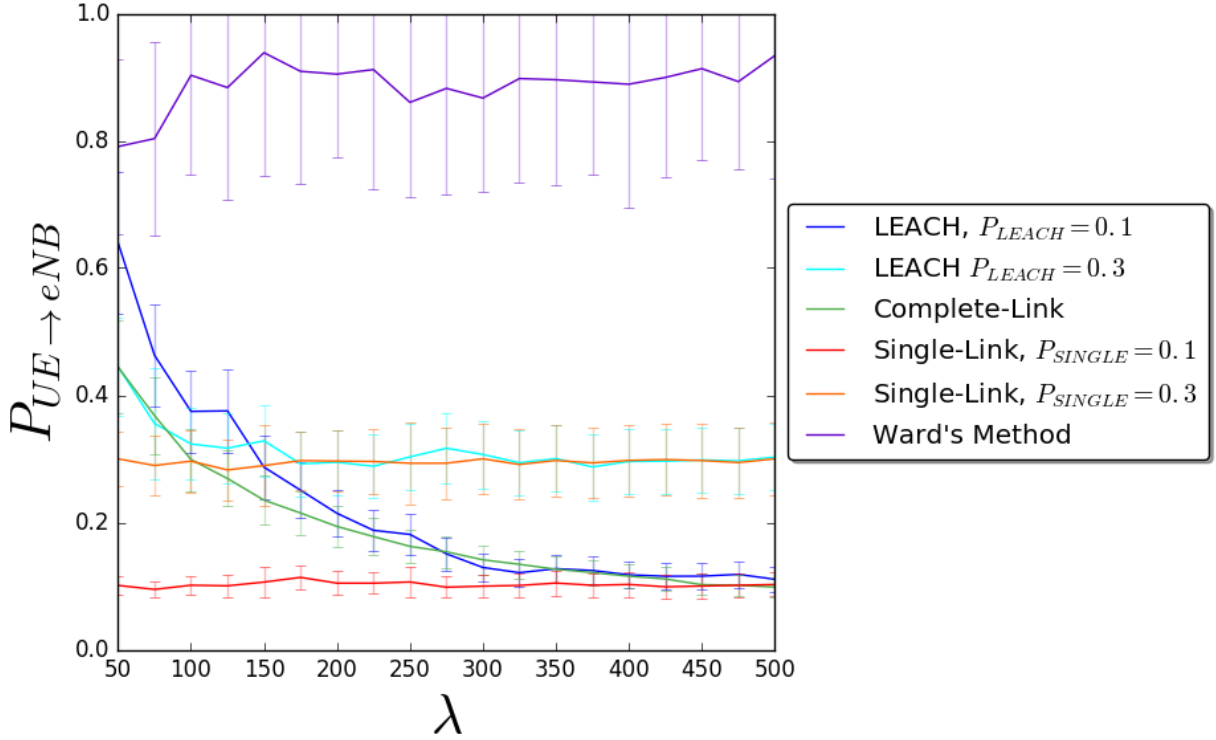
Despite this, the few D2D connections that do exist exhibit a similar behavior than the others in terms of **mean channel utilization rate**  $\bar{\rho}_{channel}$  (figure 4.8b) and **total resource efficiency** (figure 4.8c). The high magnitude of the levels of resource efficiency, although initially impressive can be easily disregarded: a very low number of D2D connections will make on average better use of all available D2D resources simply due to the fact that there are fewer elements between which to share the resource pool.

The low amount of connections is only highlighted by the bizarre **mean UE drop ratio**  $\bar{\theta}_{drops}$  curve of figure 4.8d. With a low number of D2D connections per cluster and, as mentioned, more resources available for each of those links, drops become a non-issue and hit 0 quickly.

(a) % of UEs connecting to eNB  $P_{UE \rightarrow eNB}$ (b) Mean channel utilization rate  $\bar{Q}_{channel}$ 

(c) Total resource efficiency

(d) Mean UE drop ratio  $\bar{\theta}_{drops}$ Figure 4.8: Behavior of Ward's method compared to  $\lambda$

Figure 4.9: Comparison: % of UEs connecting to eNB  $P_{UE \rightarrow eNB}$ 

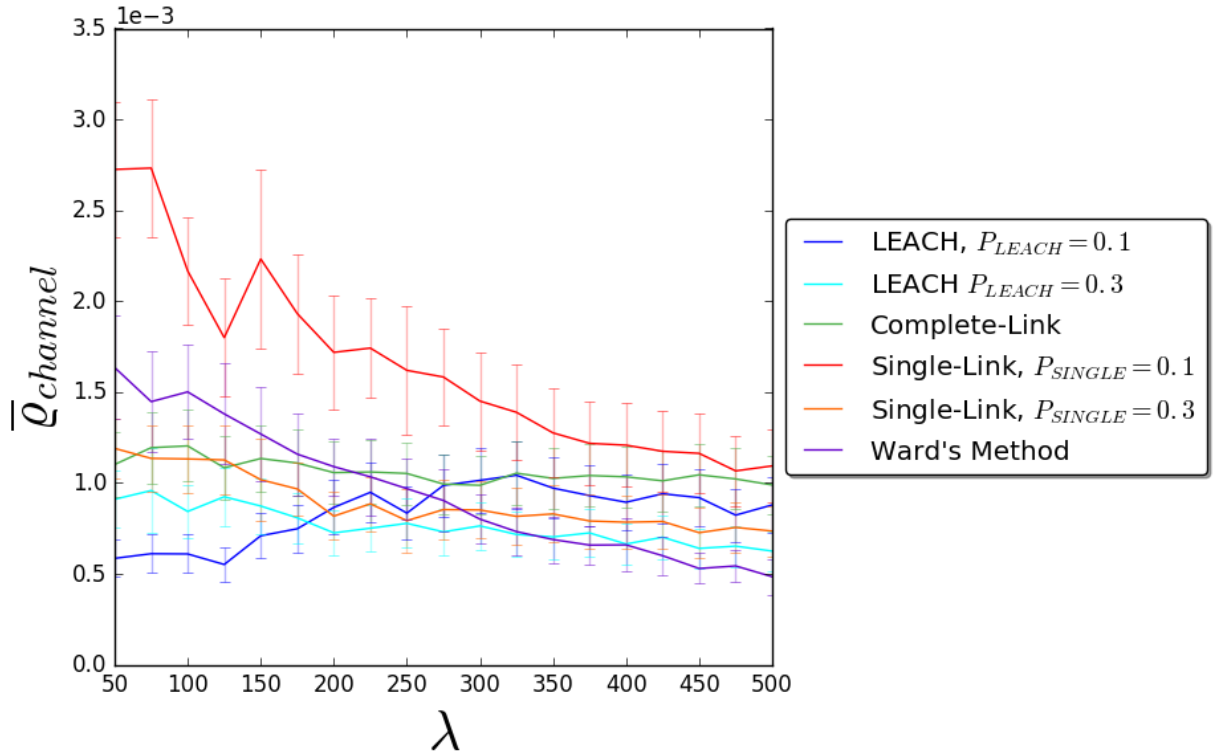
## 4.4 Comparison

### 4.4.1 Percentage of UEs connecting to eNB

As can be verified in 4.9, most clustering schemes perform their duty of restricting the amount of connections that reach the eNB by using D2D links. The plots corresponding to Single-Link, as mentioned before, do not contain much information by themselves, but they become more intriguing when comparing them to their LEACH-spawned brethren. Lower values of  $P_{LEACH}$  appear to necessitate higher densities of devices to reach their desired percentage of connections, establishing Single-Link as a better alternative when the levels of  $P_{UE \rightarrow eNB}$  are of the essence and particularly in lower densities.

Complete-Link on the other hand, performs surprisingly similarly to LEACH with  $P_{LEACH} = 0.1$ . Despite better values of  $P_{UE \rightarrow eNB}$  at lower densities, the fact that Complete-Link requires much more information from the network before it can compute clusters makes it seem more lackluster. This is only highlighted by the fact that, through most values of  $\lambda$ , Single-Link shows consistently lower  $P_{UE \rightarrow eNB}$ .

The easy scalability of both LEACH and Single-Link to suit a desired  $P_{UE \rightarrow eNB}$  should be of note. In this way, the eNB could conceivably “change” algorithms depending on the

Figure 4.10: Comparison: Mean channel utilization rate  $\bar{Q}_{channel}$ 

load it is experiencing at a particular moment, effectively allocating available resources dynamically. This could be integrated into observations about daily data traffic patterns, restricting the desired amount of aggregated data requests in particularly busy hours and relaxing it in others.

As previously expressed in section 4.3.3, this graph particularly evidences the inadequacy of Ward's method as a clustering scheme in our simulated scenario, at least the way we defined it. It is conceivable that Ward's method could serve its purpose in situations where there is a relative wealth of available cellular resources, diminishing the need for spectrum reutilization through D2D. This scenario, however, does not correspond with either our simulations nor our expectations of the future development of wireless networking. Even then, simpler mechanisms, such as LEACH with a particularly high  $P_{LEACH}$  could meet this objective without the relative complexity of Ward's method.



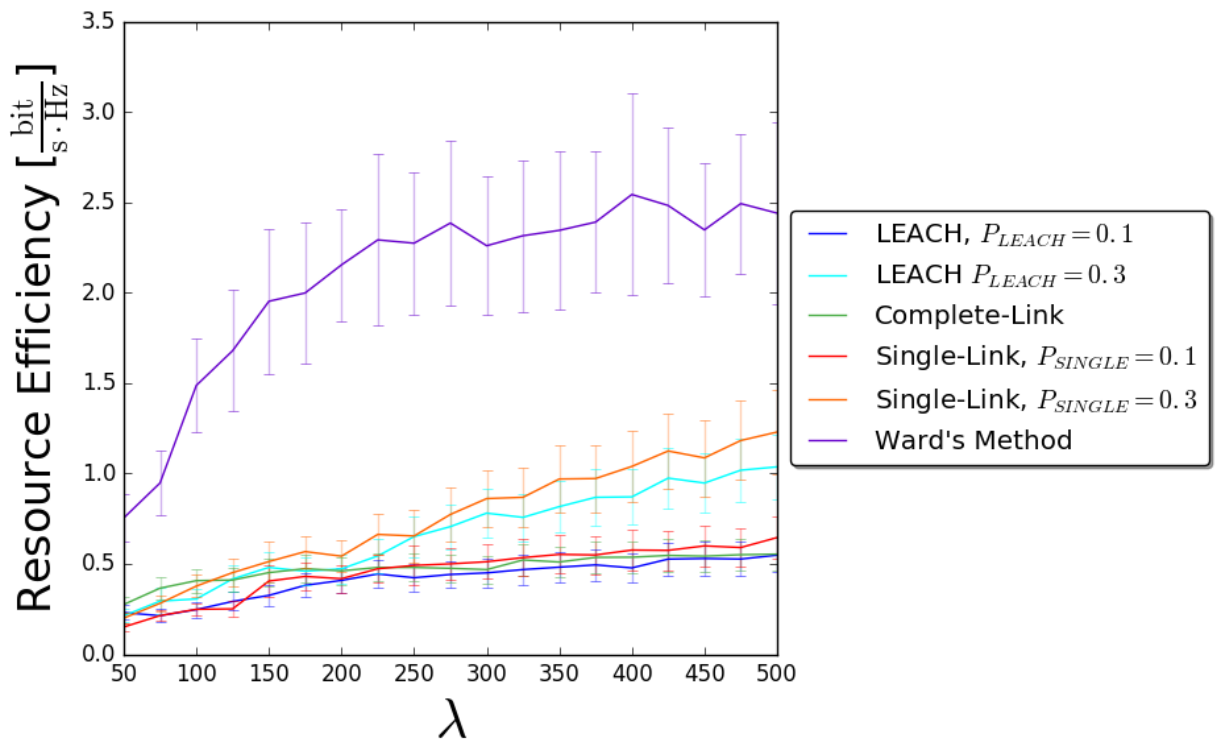
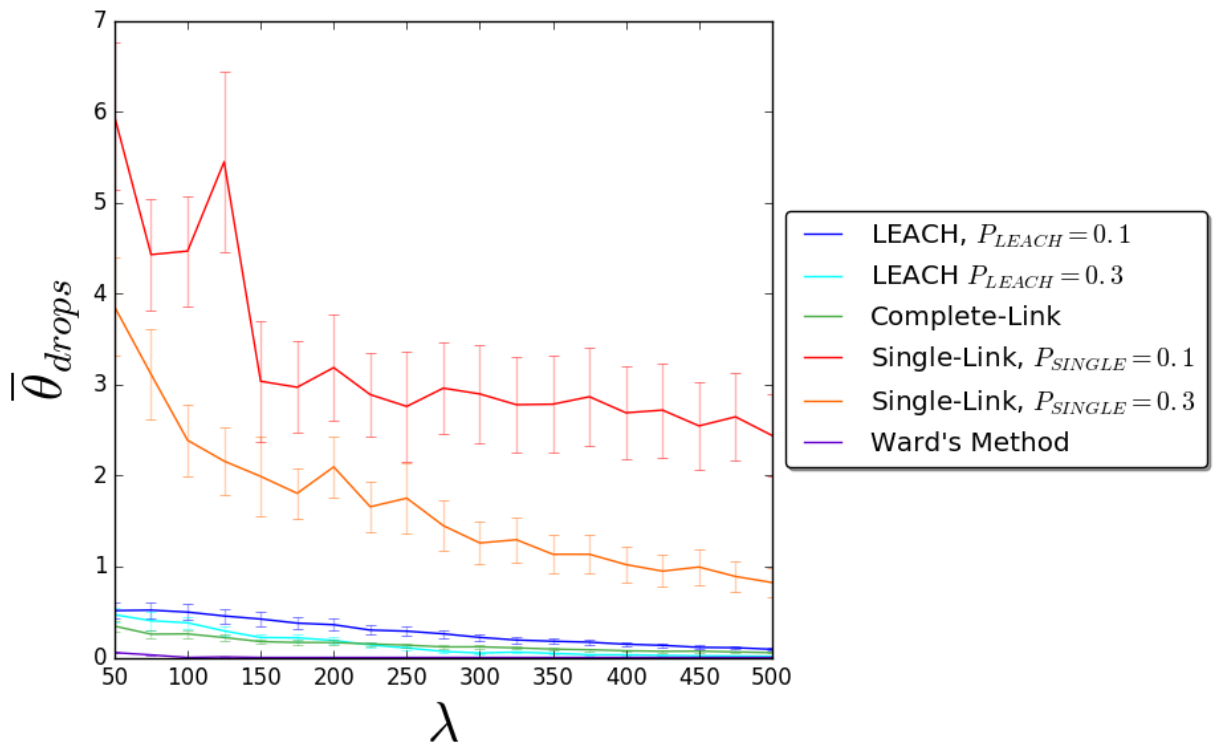


Figure 4.11: Comparison: Total resource efficiency

Figure 4.12: Comparison: Mean UE drop ratio  $\bar{\theta}_{drops}$

# Chapter 5

## Conclusions and Outlook

The thesis is concluded here. The considered problem is repeated. The contribution of this work is highlighted and the results are recapitulated. Remaining questions are stated and ideas for future work are expressed.

A big open question is of course, the decision to fix the arrival rate  $\lambda_A$ . If the data being transferred is highly correlated and includes redundancy, as is often the case with WSNs, then lower request creation rate with higher number of devices makes sense: the frequency of the information that needs to be transmitted can afford to be lower. However, our simulation scenario was thought out to have very disparate data sources, making it intrinsically different from the WSN scenario. More research is needed with a  $\lambda_A$  defined at the UE and not at the cluster head, to better evaluate the negative (and even potentially positive) effect that increased interference both within and without the cluster may cause. Thankfully this sort of adjustment seems relatively simple to make and integrate into the current models for future work.

This leads us to the successful establishment of a simulation environment for evaluation of LTE-A and especially D2D, one of the main goals of this thesis. Despite much trial and error, the work presented here will, in the mind of the author, make a positive impact in his future investigative efforts, especially in the context of already ongoing studies in the institute.

The way for future work seems relatively clear:

MODEL AT ENB CHANGING LAMBDA INCORPORATION OF OTHER KINDS OF AGGREGATION (MULTI HOP)

# Appendix A

## Notation and Abbreviations

Mean point density	$\lambda$
Breakpoint distance	$d'_{BP}$
Center frequency	$f_c$
Effective height (of UE or BS)	$h'_{BS/UE}$
Wavelength	$\lambda_{WL}$
Pathloss	$PL$
Power decay constant	$n_i$
Decorrelation distance	$d_{corr}$
Request arrival rate	$\lambda_A$
Power (transmission, received or noise)	$P_{Tx/Rx/N}$
Noise density	$N_0$
Noise factor	$NF$
Bandwidth	$W$
Number of preambles for D2D communication	$m$
Duration (slot or total)	$T_{slot/total}$
LEACH cluster head activation probability	$P_{LEACH}$
LEACH cluster head activation threshold value	$T(n)$
Mean channel utilization rate	$\bar{\varrho}_{channel}$
Resource efficiency of a network	$RE(\mathcal{G})$
D2D link (resource efficiency)	$w_{ij}$
Fraction of available resources used	$\eta_{ij}$
Total available resources	$\mathcal{R}(\mathcal{G})$
Mean UE drop ratio	$\bar{\theta}_{drops}$

Table A.1: Important symbols and placeholders used in this work, by order of appearance

BS	Base Station
BER	Bit-Error-Rate
CH	Cluster Head
D2D	Device-to-Device
eNodeB	Evolved Node B or E-UTRAN Node B
IMT-A	International Mobile Telecommunications-Advanced
IoT	Internet of Things
ITU	International Telecommunication Union
LOS	Line-of-Sight
LTE	Long Term Evolution
MCS	Modulation and Coding Scheme
METIS	Mobile and wireless communications Enablers for the Twenty-twenty Information Society
MTC	Machine Type Communication
NLOS	Non-Line-of-Sight
O2I	Outside-to-Inside
O2O	Outisde-to-Outside
PDCCH	Physical Downlink Control Channel
PDSCH	Physical Downlink Shared Channel
PPP	Poisson Point Process
PRB	Physical Resource Block
PUCCH	Physical Uplink Control Channel
PUSCH	Physical Uplink Shared Channel
QoS	Quality of Service
RA	Random Access
RACH	Random Access Channel
SINR	Signal-to-Interference-and-Noise-Ratio
SNR	Signal-to-Noise-Ratio
UE	User Equipment
WINNER+	Wireless World Initiative New Radio+
WSN	Wireless Sensor Network
3GPP	Third Generation Partership Project

Table A.2: Abbreviations used in this work

# List of Figures

2.1	Detail of the Random Access Procedure, [LAAZ14]	8
2.2	Example of D2D Clustering in a network [WSH <sup>+</sup> 13]	10
3.1	Example of a PPP with $\lambda = 200$	12
3.2	Comparison between two Manhattan Grids	14
3.3	Calculation of NLOS path	16
3.4	Visualization of NLOS path with intersection acting as relay node	17
3.5	Shadow Fading values before and after correlation adjustment	18
3.6	Sample clustering as a result of Ward's Method [Sha09]	24
4.1	Behavior of LEACH compared to $P_{LEACH}$ and $\lambda$	30
4.2	LEACH: Percentage of UEs connecting to eNB $P_{UE \rightarrow eNB}$ in relation to mean point density $\lambda$	31
4.3	LEACH: Mean channel utilization rate $\bar{\varrho}_{channel}$ in relation to mean point density $\lambda$	32
4.4	LEACH: Total resource efficiency in relation to mean point density $\lambda$	32
4.5	LEACH: Mean UE drop ratio $\bar{\theta}_{drops}$ in relation to mean point density $\lambda$	33
4.6	Behavior of Complete-Link clustering compared to $\lambda$	34
4.7	Behavior of Single-Link clustering compared to $\lambda$	36
4.8	Behavior of Ward's method compared to $\lambda$	38
4.9	Comparison: % of UEs connecting to eNB $P_{UE \rightarrow eNB}$	39
4.10	Comparison: Mean channel utilization rate $\bar{\varrho}_{channel}$	40
4.11	Comparison: Total resource efficiency	41
4.12	Comparison: Mean UE drop ratio $\bar{\theta}_{drops}$	42

# List of Tables

3.1	Manhattan grid parameters . . . . .	14
4.1	Parameters relevant for pathloss calculation . . . . .	26
4.2	Parameters relevant for random access and interference . . . . .	26
A.1	Important symbols and placeholders used in this work, by order of appearance	44
A.2	Abbreviations used in this work . . . . .	45

# Bibliography

- [3Gp09] 3Gpp. TR 136 942 - V8.1.0 - LTE; Evolved Universal Terrestrial Radio Access (E-UTRA); Radio Frequency (RF) system scenarios (3GPP TR 36.942 version 8.1.0 Release 8). 0:0–84, 2009.
- [3rd11] 3rd Generation Partnership Project;. Ran Improvements for Machine-type Communications [RP-100330], 2011.
- [3rd12] 3rd Generation Partnership Project;. Evolved Universal Terrestrial Radio Access; LTE Coverage Enhancements (Release 11) [36-824]. 0(Release 11), 2012.
- [3rd14] 3rd Generation Partnership Project;. Study on LTE Device to Device Proximity Services; Radio Aspects (Release 12) [36843-c01], 2014.
- [ATN14] M Mehdi Afsar and Mohammad H Tayarani-N. Clustering in sensor networks: A literature survey. *Journal of Network and Computer Applications*, 46:198–226, 2014.
- [Cox12] Christopher Cox. *AN INTRODUCTION TO LTE: LTE, LTE-Advance, SAE and 4G Mobile Communications*. 2012.
- [DGK<sup>+</sup>13] P. Demestichas, A. Georgakopoulos, D. Karvounas, K. Tsagkaris, V. Stavroulaki, J. Lu, C. Xiong, and J. Yao. 5g on the horizon: Key challenges for the radio-access network. *IEEE Vehicular Technology Magazine*, 8(3):47–53, Sept 2013.
- [ELLS11] Brian S. Everitt, Sabine Landau, Morven Leese, and Daniel Stahl. *Cluster Analysis*, volume 14. 2011.
- [EMIA13] M Cenk Erturk, Sayandev Mukherjee, Hiroyuki Ishii, and Huseyin Arslan. Distributions of transmit power and SINR in device-to-device networks. *IEEE Communications Letters*, 17(2):273–276, 2013.
- [FDM<sup>+</sup>12] G. Fodor, E. Dahlman, G. Mildh, S. Parkvall, N. Reider, G. Miklós, and Z. Turányi. Design aspects of network assisted device-to-device communications. *IEEE Communications Magazine*, 50(3):170–177, March 2012.



- [FSA04] Ingo Forkel, Marc Schinnenburg, and Markus Ang. Generation of two-dimensional correlated shadowing for mobile radio network simulation. *WPMC, sep*, (February):10–14, 2004.
- [HCB00] Wendi Rabiner Heinzelman, Anantha Chandrakasan, and Hari Balakrishnan. Energy-efficient communication protocol for wireless microsensor networks [LEACH]. *Proceedings of the 33rd Annual Hawaii International Conference on System Sciences*, pages 3005–3014, 2000.
- [HSK<sup>+</sup>10] Petteri Heino, Essi Suikkanen, Esa Kunnari, Juha Meinilä, Pekka Kyösti, Lassi Hentilä, Tommi Jämsä, and Milan Narandžić. D5.3: WINNER+ Final Channel Models. 1(107):107, 2010.
- [JYZ09] Congfeng Jiang, Daomin Yuan, and Yinghui Zhao. Towards Clustering Algorithms in Wireless Sensor Networks-A Survey. *2009 IEEE Wireless Communications and Networking Conference (WCNC2009)*, pages 1–6, 2009.
- [Kee] Holger Paul Keeler. Studying the SINR process of the typical user in Poisson networks by using its factorial moment measures . pages 1–27.
- [Kee16] Paul Keeler. Notes on the Poisson point process. pages 1–33, 2016.
- [KK14a] Markus Klugel and Wolfgang Kellerer. Introduction of an efficiency metric for device-to-device communication in cellular networks. *IEEE Vehicular Technology Conference*, 2014.
- [KK14b] Markus Klügel and Wolfgang Kellerer. On the feasibility of frequency reuse and spatial occupation in wireless device-to-device networks. *2014 IEEE International Black Sea Conference on Communications and Networking, Black-SeaCom 2014*, pages 154–159, 2014.
- [LAAZ14] A Laya, L Alonso, and J Alonso-Zarate. Is the Random Access Channel of LTE and LTE-A Suitable for M2M Communications? A Survey of Alternatives. 16(1):4–16, 2014.
- [LLA15] Namyoong Lee, Xingqin Lin, and Jeffrey G Andrews. Power Control for D2D Underlaid Cellular Networks: Modeling, Algorithms and Analysis. *IEEE Journal on Selected Areas in Communications*, 33(1):1–12, 2015.
- [LQL13] Ying Liao, Huan Qi, and Weiqun Li. Load-balanced clustering algorithm with distributed self-organization for wireless sensor networks. *IEEE Sensors Journal*, 13(5):1498–1506, 2013.
- [LWW<sup>+</sup>14] Andres Laya, Kun Wang, Ashraf Awadelkarim Widaa, Jesus Alonso-Zarate, Jan Markendahl, Luis Alonso, and Francisco J. Díaz Borbón. Device-to-device communications and small cells: Enabling spectrum reuse for dense networks. *IEEE Wireless Communications*, 21(4):98–105, 2014.

- [MKJH09] Juha Meinilä, Pekka Kyösti, Tommi Jämsä, and Lassi Hentilä. WINNER II Channel Models. *Radio Technologies and Concepts for IMT-Advanced*, 1(82):39–92, 2009.
- [Mw15] Mobile and wireless communications Enablers for the Twenty-twenty Information Society. Deliverable D1.4 METIS Channel Models. 2015.
- [NXW11] D Niyato, Lu Xiao, and Ping Wang. Machine-to-machine communications for home energy management system in smart grid. *Communications Magazine, IEEE*, 49(4):53–59, 2011.
- [PCZZ16] Michele Polese, Marco Centenaro, Andrea Zanella, and Michele Zorzi. On the Evaluation of LTE Random Access Channel Overload in a Smart City Scenario. 3, 2016.
- [RCCM15] Andre Riker, Eduardo Cerqueira, Marilia Curado, and Edmundo Monteiro. A Two-Tier Adaptive Data Aggregation Approach for M2M Group-Communication. *IEEE Sensors Journal*, 16(c):1, 2015.
- [Rep09] Report ITU-R M.2135-1. Guidelines for evaluation of radio interface technologies for IMTAdvanced. *Evaluation*, 93(3), 2009.
- [Sha09] Cosma Shalizi. Distances between Clustering , Hierarchical Clustering. *Data Mining*, (September):36–350, 2009.
- [SOIJ15] H Shariatmadari, P Osti, S Iraj, and R Jäntti. Data Aggregation in Capillary Networks for Machine-to-Machine Communications. *Proc. IEEE Personal, Indoor and Mobile Radio Communications (PIMRC) – Workshop on M2M Communications: Challenges, Solutions and Applications*, pages 1100–1105, 2015.
- [SRI<sup>+</sup>15] Hamidreza Shariatmadari, Rapeepat Ratasuk, Sassan Iraj, Andrés Laya, Tarik Taleb, Riku Jäntti, and Amitava Ghosh. Machine-type communications: current status and future perspectives toward 5G systems. *IEEE Communications Magazine*, 53(9):10–17, 2015.
- [War63] Joe H. Ward. Hierarchical grouping to optimize an objective function, 1963.
- [WHS12a] Shih-en Wei, Hung-yun Hsieh, and Hsuan-jung Su. Enabling Dense Machine-to-Machine Communications through Interference-Controlled Clustering. pages 774–779, 2012.
- [WHS12b] Shih-en Wei, Hung-yun Hsieh, and Hsuan-jung Su. Joint Optimization of Cluster Formation and Power Control. pages 5512–5518, 2012.
- [WSH<sup>+</sup>13] Sen Hung Wang, Hsuan Jung Su, Hung Yun Hsieh, Shu Ping Yeh, and Minnie Ho. Random access design for clustered wireless machine to machine networks. *2013 1st International Black Sea Conference on Communications and Networking, BlackSeaCom 2013*, pages 107–111, 2013.